© 2015. Published by The Company of Biologists Ltd | Journal of Cell Science (2015) 128, 1294–1307 doi:10.1242/jcs.155143

RESEARCH ARTICLE

Human FAM154A (SAXO1) is a microtubule-stabilizing protein specific to cilia and related structures

Denis Dacheux[1,2,3], Benoit Roger[1,2], Christophe Bosc[4,5], Nicolas Landrein[1,2], Emmanuel Roche[1,2], Lucie Chansel[6], Thomas Trian[7,8], Annie Andrieux[4,5,9], Aline Papaxanthos-Roche[6], Roger Marthan[7,8], Derrick R. Robinson[1,2] and Mélanie Bonhivers[1,2,*]

ABSTRACT

Cilia and flagella are microtubule-based organelles present at the surface of most cells, ranging from protozoa to vertebrates, in which these structures are implicated in processes from morphogenesis to cell motility. In vertebrate neurons, microtubule-associated MAP6 proteins stabilize cold-resistant microtubules through their Mn and Mc modules, and play a role in synaptic plasticity. Although centrioles, cilia and flagella have cold-stable microtubules, MAP6 proteins have not been identified in these organelles, suggesting that additional proteins support this role in these structures. Here, we characterize human FAM154A (hereafter referred to as hSAXO1) as the first human member of a widely conserved family of MAP6-related proteins specific to centrioles and cilium microtubules. Our data demonstrate that hSAXO1 binds specifically to centriole and cilium microtubules. We identify, *in vivo* and *in vitro*, hSAXO1 Mn modules as responsible for microtubule binding and stabilization as well as being necessary for ciliary localization. Finally, overexpression and knockdown studies show that hSAXO1 modulates axoneme length. Taken together, our findings suggest a fine regulation of hSAXO1 localization and important roles in cilium biogenesis and function.

KEY WORDS: MAP6, Microtubule, Microtubule-stabilizing protein, Cilium, Centriole, Basal body, Flagellum, Axoneme, Cytoskeleton, Spermatozoon, Epithelial cell

INTRODUCTION

Primary cilia are present on the surface of most human cells, and motile cilia are present in tracheal epithelium, ependyma, epididymis, oviduct epithelium, embryonic node and sperm (in the latter case they are called flagella). Cilia are implicated in numerous processes, from morphogenesis to cell motility, and their dysfunction is associated with ciliopathies such as polycystic kidney disease and male infertility (Fliegauf et al., 2007; Oh and Katsanis, 2012). Motile and non-motile cilia contain a cytoskeleton, which consists of a complex and essential microtubule-based-structure called the axoneme. Axoneme biogenesis is initiated from the basal bodies, which themselves are centriole-related structures (Carvalho-Santos et al., 2011; Marshall, 2009). The axoneme is composed of nine doublet microtubules (MTs) surrounding a central pair for most motile cilia (9+2), whereas no central pair is present for most immotile cilia (9+0) (Takeda and Narita, 2012).

The dynamics of assembly and disassembly of tubulin polymers (MTs) is tightly regulated, in part by either post-translational modifications (PTMs) or their association with proteins such as microtubule-associated proteins (MAPs), tektins and ribbon filaments (Amos and Schlieper, 2005; Bobinnec et al., 1998; Debec et al., 2010; Grimes and Gavin, 1987; Hinchcliffe and Linck, 1998; Janke et al., 2008; Quinones et al., 2011; Steffen and Linck, 1988). In vertebrates, most MTs will disassemble at low temperature (Lieuvin et al., 1994; Snyder and McIntosh, 1976). In some cases, however, the resistance of some MTs to cold-induced depolymerization is observed to be largely due to their association with the class of MAPs known as MAP6 [previously known as stable tubule only polypeptide (STOP)] and MAP6d1 (the latter protein shares significant homology with neuronal MAP6 over the N-terminal domain and a microtubule-stabilizing domain) (Bosc et al., 2003; Brinkley and Cartwright, 1975; Gory-Fauré et al., 2006; Margolis et al., 1986; Margolis et al., 1990). MAP6 proteins are calmodulin-regulated proteins expressed in neurons, astrocytes, oligodendrocytes, fibroblasts and several tissues (including heart, muscle, lung and testis) (Bosc et al., 2001; Denarier et al., 1998; Galiano et al., 2004; Gory-Fauré et al., 2006; Guerrero et al., 2010; Pirollet et al., 1989). MAP6 proteins stabilize MTs through two types of MT-binding modules – a central Mc module repeat (1–6 modules) that conveys resistance to cold-induced disassembly, and an Mn module repeat (1–3 modules) that conveys resistance to both cold- and nocodazole-induced disassembly. Although the Mn modules are well conserved in vertebrate MAP6 proteins, the Mc modules are only found in mammals (Bosc et al., 2001; Bosc et al., 2003). *In vitro* biophysical studies have demonstrated that module Mn1 and Mn2 of MAP6 are able to bind to and stabilize MTs upon cold treatment by bridging tubulin heterodimers (Lefèvre et al., 2013). MAP6 proteins also share an N-terminal cysteine-rich sequence that targets the proteins to the Golgi complex when palmitoylated (Bosc et al., 2003; Gory-Fauré et al., 2006).

The physiological role of the MAP6 proteins in vertebrates is still unclear, but it is known that MAP6 depletion in mice leads to synaptic defects and severe disorders that are reminiscent of

[1]University Bordeaux, Microbiologie Fondamentale et Pathogénicité, UMR 5234, F-33000 Bordeaux, France. [2]CNRS, Microbiologie Fondamentale et Pathogénicité, UMR 5234, F-33000 Bordeaux, France. [3]Institut Polytechnique de Bordeaux, Microbiologie Fondamentale et Pathogénicité, UMR 5234, F-33000 Bordeaux, France. [4]INSERM, Centre de Recherche U836, F-38000, Grenoble, France. [5]University Grenoble Alpes, Grenoble Institut des Neurosciences, F-38000, Grenoble, France. [6]CHU de Bordeaux, Centre Aliénor d'Aquitaine, Laboratoire de Biologie de la Reproduction, F-33000 Bordeaux, France. [7]University Bordeaux, Centre de Recherche Cardio-thoracique de Bordeaux, U1045, F-33000 Bordeaux, France. [8]INSERM, Centre de Recherche Cardio-thoracique de Bordeaux, U1045, F-33000 Bordeaux, France. [9]CEA, Institut de Recherches en Technologies et Sciences pour le Vivant, GPC, F-38000 Grenoble, France.

*Author for correspondence (melanie.bonhivers@u-bordeaux.fr)

Received 14 April 2014; Accepted 5 February 2015

Journal of Cell Science

Journal of Cell Science (2015) 128, 1294–1307 doi:10.1242/jcs.155143

schizophrenia-like symptoms (Andrieux et al., 2002; Volle et al., 2013). MAP6 is also involved in crosstalk between the actin and MT cytoskeleton networks (Baratier et al., 2006), and between intermediate filaments and MTs, as well as in the dendritic trafficking of lysosomes through its interaction with Bmcc1s (an intermediate-filament- and MT-associated protein involved in the regulation of cytoskeleton dynamics in mouse brain) (Arama et al., 2012). MAP6 also interacts with TMEM106B (a late endosome and lysosomal protein in neurons) (Schwenk et al., 2014). Finally, MAP6 is involved in MT stabilization during temperature decrease, acting as a temperature sensor (Delphin et al., 2012).

In mammals, centrioles, cilia and flagella have cold-stable microtubules (Behnke and Forer, 1967; Bornens, 2002; Grimes and Gavin, 1987; Hesketh et al., 1984; Quinones et al., 2011), but MAP6 proteins are most likely not involved in their stabilization as they have not been localized to these structures, although MAP6 was annotated as a centrosomal protein (Nogales-Cadenas et al., 2009) and *Map6d1* gene expression is upregulated in multi-ciliated tracheal epithelial cells (Hoh et al., 2012). The molecular component responsible for the cold and nocodazole resistance of these MTs has thus not been identified.

We have recently identified a MAP6-related family of proteins that we called the SAXO proteins (for stabilizer of axonemal microtubules) (Dacheux et al., 2012). In contrast to the distribution of MAP6 and MAP6d1 genes, which are present only in vertebrates, genes that encode SAXO1 and SAXO2 are present in eukaryotes from protozoa to mammals, but only in ciliated or flagellated organisms. The first member of this family was characterized in the parasitic flagellated pathogen *Trypanosoma brucei* (hereafter referred to as tSAXO). tSAXO stabilized MTs upon cold or nocodazole treatments, and stabilization was shown to be mediated through the Mn modules. That work also demonstrated that tSAXO is an axoneme-specific protein. RNA interference (RNAi)-mediated knockdown of its expression impaired flagellar beating and cell mobility, thus suggesting a role in flagellum motility. In mammals, we have identified two genes that encode SAXO1 and SAXO2, corresponding to the uncharacterized *FAM154A* and *FAM154B* genes, respectively. The identification of tSAXO in *T. brucei* flagella and of the SAXO protein family specific to ciliated or flagellated organisms, as well as human and rodent SAXO1 in mature sperm (by mass spectrometry) (Baker et al., 2008a; Baker et al., 2008b; Baker et al., 2013), suggests that SAXO1 could be universally specific to cilia and the MTs of related structures.

In this work, we show that human (h) FAM154A (hereafter referred to as hSAXO1) is the first human member of a widely conserved family of MAP6-related proteins specific to cilia and related structures. Expression of recombinant versions of hSAXO1 identifies the Mn modules as necessary for MT targeting and stabilization upon cold treatment *in vivo* and *in vitro*, as well as for localization to the cilia *in vivo*. Furthermore, we demonstrate that hSAXO1 is involved in the regulation of primary cilium length. Because the localization of hSAXO1 is different depending on cell type, our results suggest specific roles in cilium biogenesis and function.

RESULTS

hSAXO1 belongs to the SAXO protein family and is related to MAP6 proteins

We used MEME analysis software to identify motifs common to hSAXO1, MAP6 and other SAXO proteins. MEME is a software tool that is used to discover novel motifs in protein sequences and to search for the occurrences of motifs in sequence databases. MEME analysis of SAXO and MAP6 proteins (from protozoa to mammals) identified that SAXO proteins possess Mn modules and an N-terminal cysteine-rich domain shared with MAP6 proteins (Fig. 1A; supplementary material Table S1). In contrast, Mc modules were identified only in MAP6 proteins, except for the apicomplexan *Toxoplasma gondii* SPM1 protein (Tran et al., 2012), which, however, has many gaps or deletions when compared with mouse Mc4. MEME analysis identified 11 Mn modules (Mn2–12) in hSAXO1, and we manually identified a twelfth module, Mn1 (Fig. 1B). For this work, we used these Mn modules to design truncated hSAXO1 constructs (Fig. 1C).

Using the C-terminal sequences (amino acids 401–474 for hSAXO1), MEME analysis identified a CPASYpsPPGy sequence within the twelfth Mn module, which is absent in MAP6 proteins but specific to vertebrate SAXO proteins (Fig. 1). The PPGy motif of hSAXO1 is similar to the PPxY motif, and these motifs are known to bind to group I WW domains. This suggests that hSAXO1 could be involved in protein–protein interactions (Dinkel et al., 2012; Hu et al., 2004). Additionally, we identified a RVxP cilium-targeting motif (R_{116}VDP) in hSAXO1 by using ELM analysis (Dinkel et al., 2014). This motif is similar to the R_6VQP of polycystin-2 and the R_{821}VSP motif of CNGB1b, both of which are axonemal proteins (Geng et al., 2006; Jenkins et al., 2006).

The human gene encoding SAXO1 is located on chromosome 9 (9p22.1), spanning 122.1 kbp, and is composed of 12 exons (supplementary material Fig. S1). Sequence analysis of genomic DNA, expressed sequence tags (ESTs) and cDNAs identified eight putative isoforms, with isoform 1 being the most represented (29 ESTs), encoding a 54.6-kDa protein (supplementary material Fig. S1; Table S2).

hSAXO1 is a ubiquitously expressed protein present in the proximal centriole and the flagellum of human sperm

Our EST database searches showed that hSAXO1 expression is ubiquitous, but that it is expressed at higher levels in testicular tissue and is linked to tissues with ciliated cells (supplementary material Table S2). End-point RT-PCR analysis using a primer pair recognizing isoforms 1, 2, 3 and 5 revealed that the transcripts are present in every human adult tissue tested (Fig. 2A). Quantitative RT-qPCR demonstrated that hSAXO1 is strongly expressed in testis and is barely detectable, although present, in all other tissues (supplementary material Fig. S2).

Because tSAXO is found in the trypanosome flagellum and because mammalian SAXO1, and *Drosophila melanogaster* (Dm)SAXO proteins were identified in mature sperm by mass spectrometry (Baker et al., 2008a; Baker et al., 2008b; Baker et al., 2013; Dorus et al., 2006; Firat-Karalar et al., 2014), we wondered whether hSAXO1 could also localize to sperm flagellar MTs. Western blot analysis of hSAXO1 in human sperm samples, using an affinity-purified rabbit polyclonal antibody raised against the last 90 amino acids of hSAXO1, revealed a single band of ≤60 KDa (Fig. 2B). This observation demonstrates that hSAXO1 is indeed expressed in mature sperm, most probably as isoform 1 (54.6 KDa) or as isoform 3 (54.1 KDa). However, as the antibody does not detect low levels of protein (as it cannot detect hSAXO1 in U-2OS or RPE1 cells by western blotting, see below), we cannot rule out that isoform 2 is being expressed.

In mature sperm cells, MTs are present in the axoneme, but also in the vestige of the distal centriole and in the proximal centriole that is associated with the centriolar adjunct

Journal of Cell Science (2015) 128, 1294–1307 doi:10.1242/jcs.155143

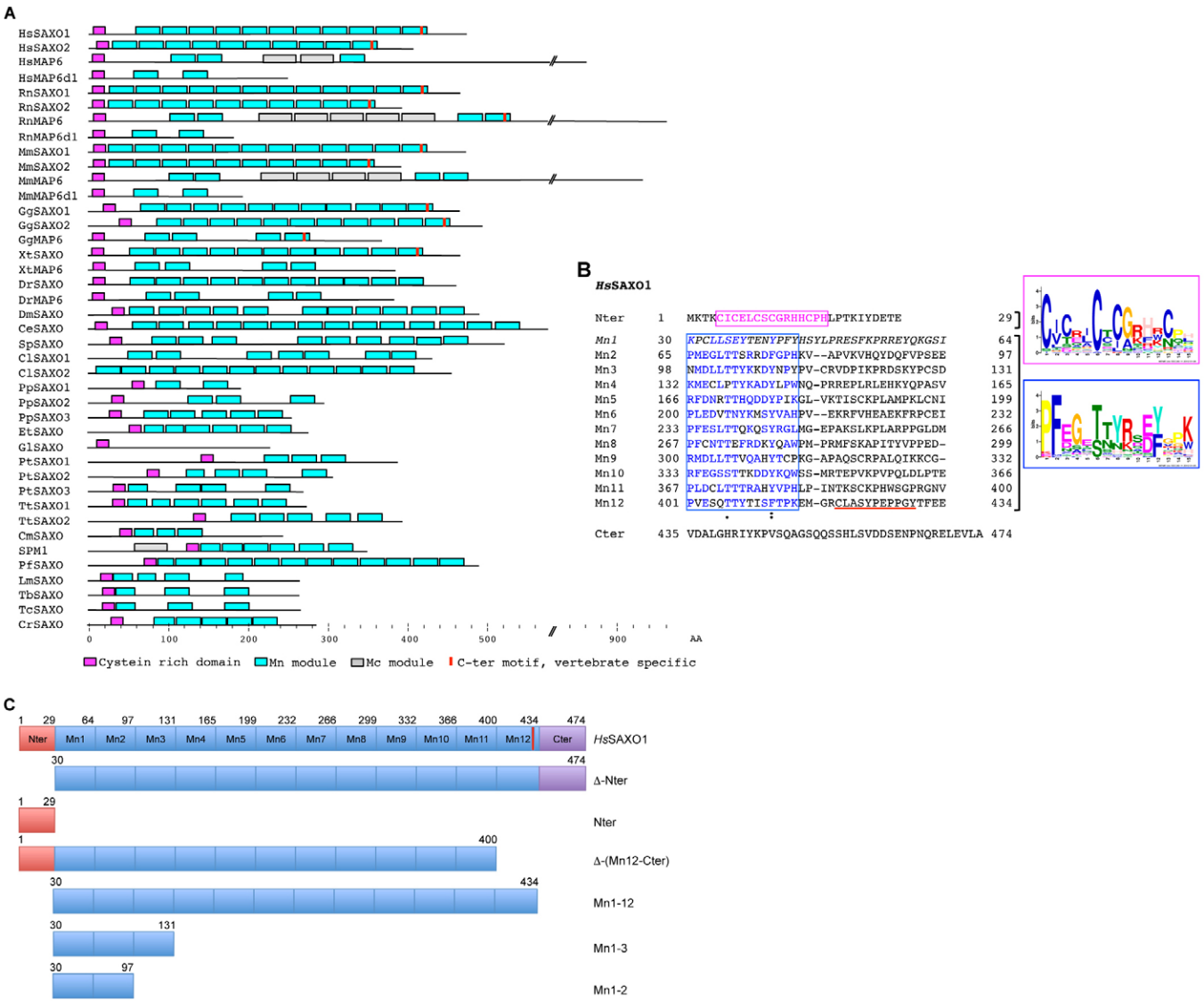

Fig. 1. Identification of shared and specific domains of SAXO and MAP6 proteins using MEME analysis. (A) MEME analysis, using MAP6 and SAXO protein primary sequences of organisms ranging from protozoa to mammals, identified a cysteine-rich domain (pink) and Mn modules (blue) that are shared by MAP6 and SAXO, as well as a SAXO vertebrate specific C-terminal motif (red rectangle). Note that the Mn modules manually annotated in Dacheux et al. (Dacheux et al., 2012) are not represented here. Protein scale in amino acid (AA) units is indicated at the bottom. The accession numbers of the sequences used in the MEME analysis are detailed in supplementary material Table S1. Hs, *Homo sapiens*; Rn, *Rattus norvegicus*; Mm, *Mus musculus*; Gg: *Gallus gallus*; Xt, *Xenopus tropicalis*; Dr, *Danio rerio*; Dm, *Drosophila melanogaster*; Ce, *Caenorhabditis elegans*; Sp, *Strongylocentrotus purpuratus*; Ci, *Ciona intestinalis*; Pp, *Physcomitrella patens*; Et, *Eimeria tenella*; Gi, *Giardia intestinalis*; Pt, *Paramecium tetraurelia*; Tt, *Tetrahymena thermophila*; Cm, *Cryptosporidium muris*; Lm, *Leishamania major*; Tb, *Trypanosoma brucei*; Tc, *Trypanosoma cruzi*; Cr, *Chlamydomonas reinhardtii*. (B) Primary sequence of the hSAXO1 protein with its Mn modules aligned using Clustal W2. The first Mn motif (*Mn1*) was identified manually as in Dacheux et al. (Dacheux et al., 2012). Pink-boxed residues in the N-terminal cysteine-rich domain correspond to the top Logo motif. Blue-boxed residues in Mn domains correspond to the bottom Logo motif. The CLASYPEPPxY motif in Mn12 is underlined. *, similar residues; **, highly conserved residues. (C) Schematic representation of recombinant hSAXO1–GFP and truncated proteins used in this study.

(Sathananthan, 2013; Sathananthan et al., 1996). Co-immunolabeling of hSAXO1 and α-tubulin on mature spermatozoa demonstrated that hSAXO1 colocalizes with MTs along the length of the axoneme from its proximal end to its distal tip (Fig. 2C). Furthermore, colocalization of tubulin and hSAXO1 occurs at the distal end of the flagellum, a region that is devoid of para-axonemal structures and where MTs can form a broom-like structure or fibrils (Markova, 2004; Pease, 1963). Interestingly, hSAXO1 immunofluorescence labeling appeared also as a dot next to the proximal end of the flagellum, corresponding to the proximal centriole. Immunoelectron microscopy of extracted spermatozoa showed that hSAXO1 localized on MTs, thus demonstrating its specificity for the axoneme and fibril MTs and not the outer dense fibers (ODFs) (Fig. 3).

hSAXO1 is a protein that localizes to the centriole, basal body and primary cilium

To investigate the cellular localization of hSAXO1 in other cell types, we immunolabeled hSAXO1 in RPE1 cells (which can

Journal of Cell Science (2015) 128, 1294–1307 doi:10.1242/jcs.155143

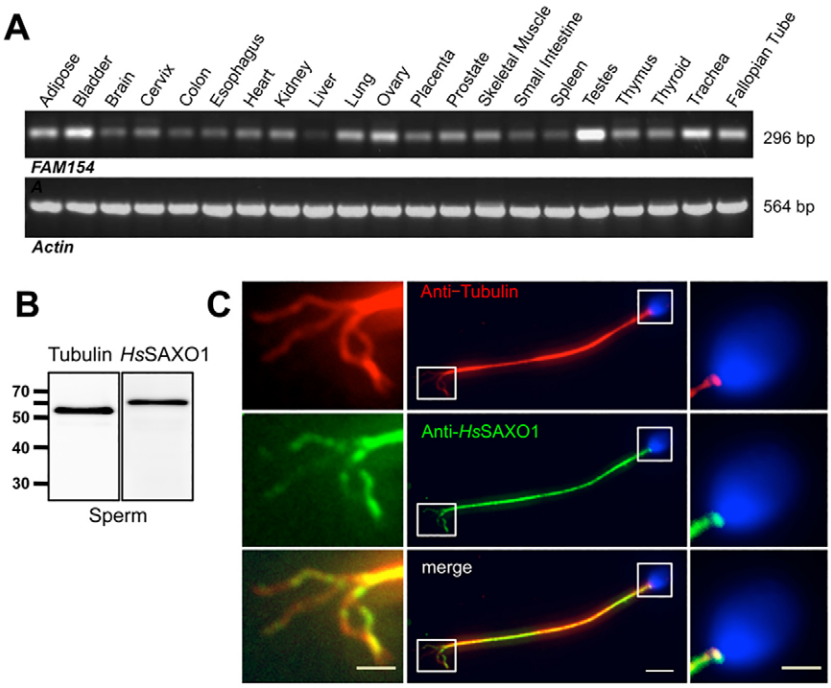

Fig. 2. hSAXO1 is a ubiquitously expressed protein and is present in human spermatozoa. (A) RT-PCR on total RNA of human adult tissues, using actin as an RNA integrity and loading control, revealed a high expression of the hSAXO1 gene in testis, whereas lower levels of transcript were observed in all other tissues. (B) Western blot on human sperm proteins using anti-tubulin and anti-hSAXO1 antibodies. (C) Immunolocalization of hSAXO1 on human sperm by immunofluorescence. Red, tubulin; green, hSAXO1. Scale bars: 2 μm (left and right panels), 5 μm (center panel).

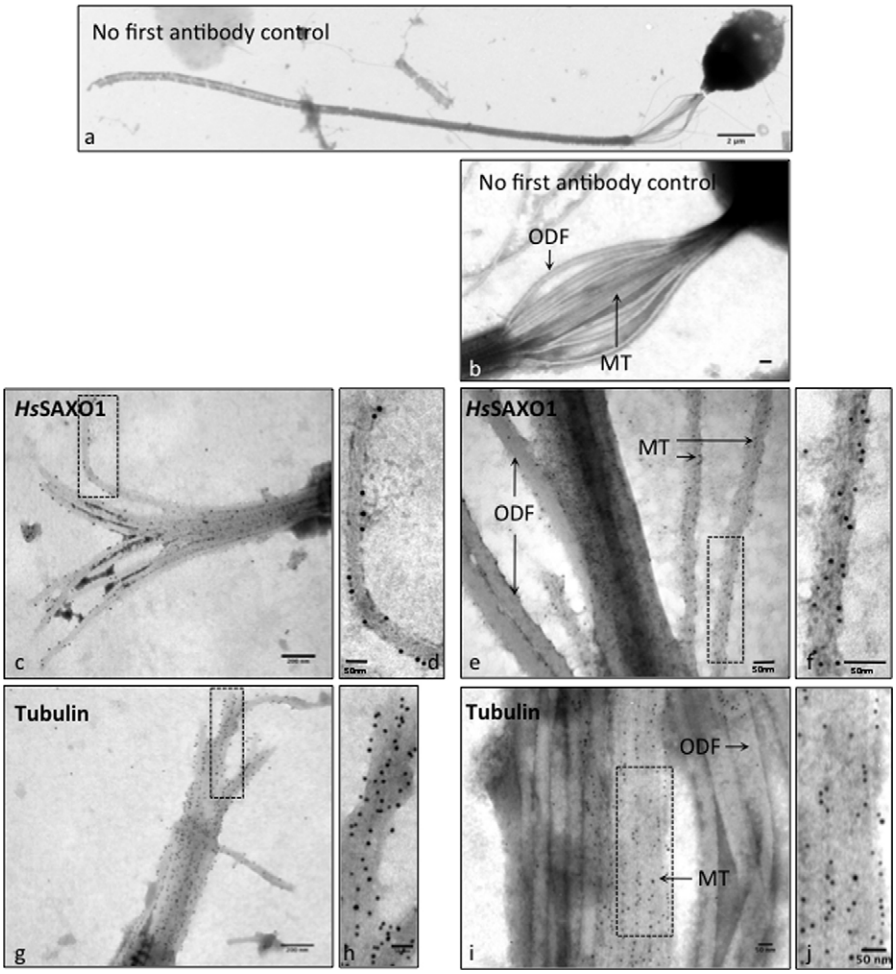

Fig. 3. hSAXO1 localizes on the microtubules of human spermatozoa. Immunogold labeling of tubulin and hSAXO1 in Triton-X-100-extracted spermatozoa. Panels a and b show the morphology of extracted spermatozoa probed with gold-conjugated secondary antibody, but no primary antibody. hSAXO1 (6-nm gold beads) localizes on MTs (c,d) and not on the ODFs (e,f), as is the case for tubulin (10-nm gold beads) (g,h,i,j). Scale bars: 2 μm (a), 200 nm (b,c,g), 50 nm (d,e,f,h,i,j). Panels d, f, h and j are enlargements of the areas indicated in c, e, g and i, respectively.

Journal of Cell Science (2015) 128, 1294–1307 doi:10.1242/jcs.155143

produce a primary cilium), in U-2OS cells (that do not produce a primary cilium), and in differentiated human bronchial epithelial cells (HBECs), which are multi-ciliated. Immunolabeling in RPE1 cells reveals that hSAXO1 localizes at the centrioles (mother and daughter) at every stage of the cell cycle, as shown with γ-tubulin co-labeling (Fig. 4A). We did not observe co-labeling of other MTs, such as the interphase microtubules, the mitotic spindle or at the midbody.

In G_0 RPE1 cells that have produced a primary cilium by 24 h of serum starvation (labeled with anti-acetylated tubulin), hSAXO1 is present at the mother and daughter basal bodies (Fig. 4A). At an early time-point of ciliogenesis, hSAXO1 was not detected in the axoneme when tested by immunofluorescence (Fig. 4A); however, after a longer period of starvation (>24 h), we observed a positive signal along the axoneme that increased with the maturation of the cilium, suggesting a correlation between the presence of hSAXO1 and the length of the cilium (Fig. 4B). Unfortunately, expression levels of hSAXO1 protein during ciliogenesis could not be quantified, as endogenous hSAXO1 was not detectable by western blotting in this cell type. Similar co-immunolabeling experiments with antibodies against tubulin or pericentrin in U-2OS cells revealed that hSAXO1 also localizes at both mother and daughter centrioles in this cell type (Fig. 4C, 37℃). This centriolar localization is preserved when most MTs (but not centriolar MTs) were depolymerized after cold (4℃) or nocodazole treatment, indicating that these treatments do not induce relocalization or redistribution of hSAXO1 (Fig. 4C).

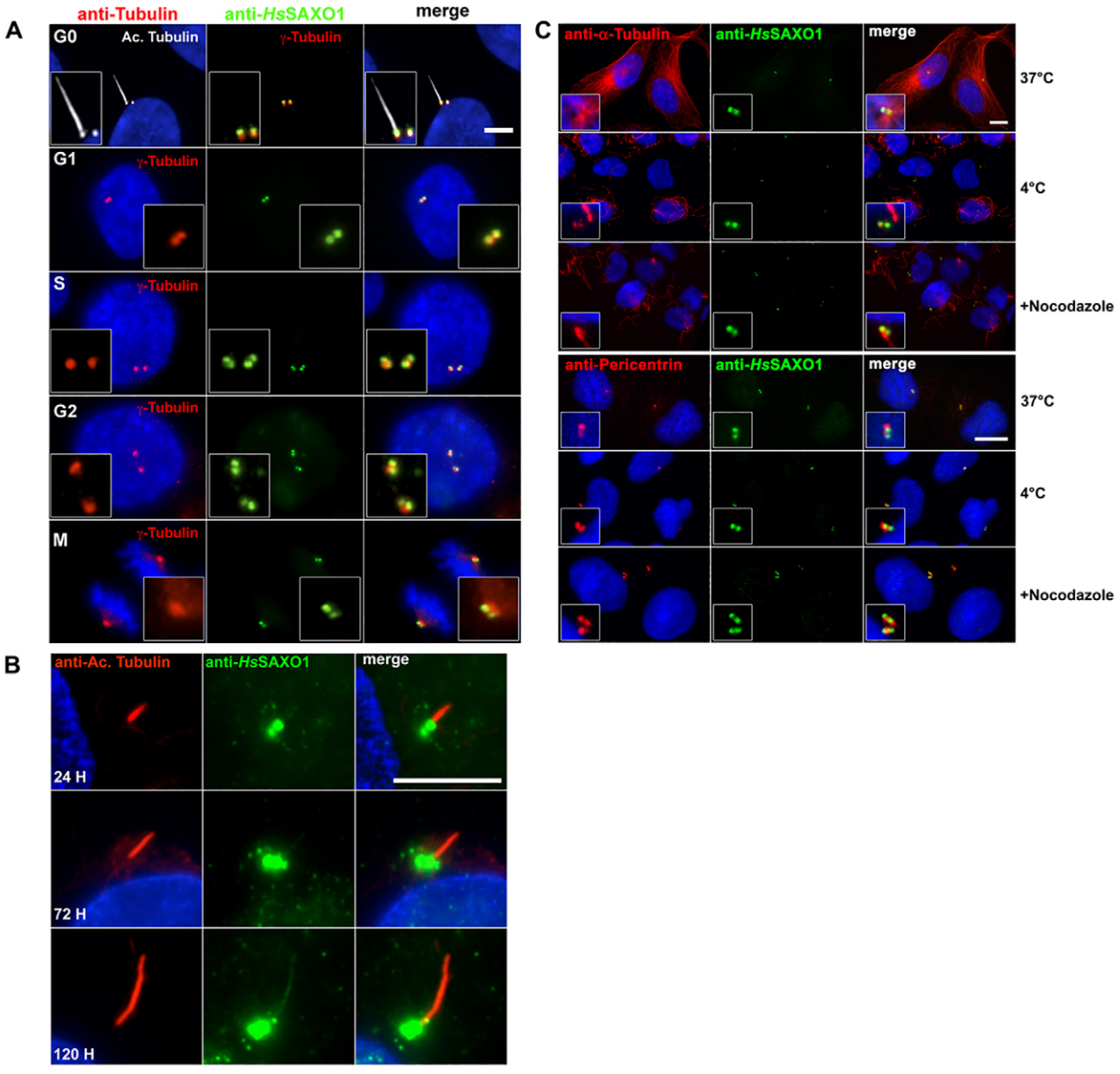

Fig. 4. hSAXO1 is a protein found in centrioles, basal bodies and cilia. (A) Immunolocalization of hSAXO1 (green) and γ-tubulin (red) in RPE1 cells in G_0, G1, S, G2 and M phases, and of acetylated (Ac.) tubulin (white) at G_0 in serum-starved cells. (B) Immunolocalization of hSAXO1 (green) and acetylated tubulin (red) in RPE1 cells incubated in low serum for 24 h, 72 h and 120 h. (C) Immunolocalization of hSAXO1 (green) with α-tubulin or pericentrin (red) in U-2OS cells. Cells were mock treated (37℃), cold treated (4℃) or nocodazole treated (+Nocodazole) before extraction and fixation. Scale bars: 5 μm (A,B), 10 μm (C).

Journal of Cell Science (2015) 128, 1294–1307 doi:10.1242/jcs.155143

We then examined the immunolocalization of hSAXO1 in HBECs, in which multi-ciliate cell differentiation was induced by exposure to an air-liquid interface (Gras et al., 2012). Acetylated tubulin and hSAXO1 co-labeling of HBECs revealed that hSAXO1 was present at the centriole of non-ciliated cells (as described above in the U-2OS and RPE1 cells), and at the basal bodies of multi-ciliated cells (supplementary material Fig. S2); however, we could not detect hSAXO1 labeling in the axoneme of HBECs, suggesting that either hSAXO1 is present only in the basal bodies or that it is below the level of detection in these cells. This observation is in accordance with the low signal level observed in the axoneme of primary cilia in RPE1 cells (Fig. 4B).

Ectopic expression in U-2OS cells characterizes hSAXO1 as a MAP6-related protein and identifies the role of the Mn modules in MT targeting, binding and stabilization

As MAP6 and tSAXO are both MT-binding and cold-stabilizing proteins, we wanted to assess the role of hSAXO1 and its domains in these functions. At 24 h after transfection of U-2OS cells, the localization of recombinant MAP6–GFP and hSAXO1–GFP was assessed by GFP immunolabeling (in whole cells). This was done at 37℃ or after a 45-min incubation at 4℃ to induce MT depolymerization (Fig. 5).

As described previously (Dacheux et al., 2012), whole-cell MAP6–GFP signal in U-2OS cells was diffuse throughout the cytoplasm at 37℃, and relocalized to cold-stabilized MTs after incubation at 4℃ (Fig. 5A). At low levels of expression, hSAXO1–GFP localized to the centrioles, thus confirming the specificity of the anti-hSAXO1 antibody and the centriole localization of hSAXO1 (Fig. 5B). This was confirmed by co-labeling with γ-tubulin (supplementary material Fig. S4). In cells expressing higher levels of hSAXO1–GFP, at 37℃ we observed additional labeling, including a dotted GFP pattern on MTs and perinuclear bundles of MTs (Fig. 5C). Co-labeling with Mitotracker Red CMXRos ruled out mitochondrion localization (data not shown). This punctate cytoplasmic localization of hSAXO1–GFP is most probably a consequence of a high level of expression compared to its endogenous expression, potentially leading to saturation of the centriole MTs and relocalization of the protein to interphase MTs (or cytosol). We took advantage of

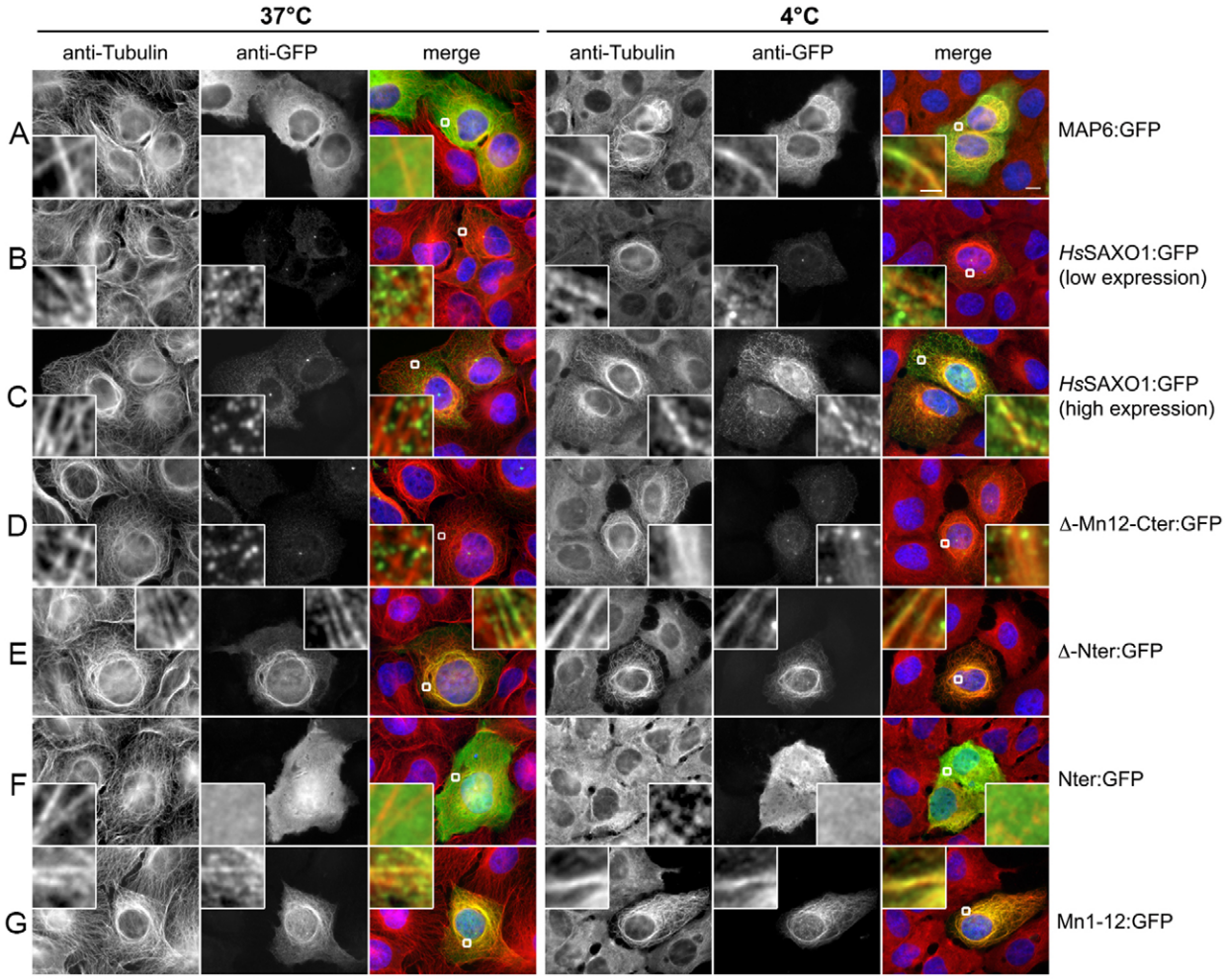

Fig. 5. Ectopic expression of truncated forms of hSAXO1 identifies functional domains. Human U-2OS cells expressing GFP-tagged MAP6 (MAP6:GFP) (A), GFP-tagged hSAXO1 (hSAXO1:GFP) (B,C) or various truncated versions of GFP-tagged hSAXO1 (D–G). In each case, transfected cells were mock treated (37℃) or cold treated (4℃) to test for MT cold stability, before being fixed and labeled with anti-tubulin (red) and anti-GFP (green) antibodies. The right columns for each temperature set are merged images. hSAXO1–GFP MT stabilization at 4℃ is seen in images B,C,D,E and G. MT stabilization is also observed in the positive control MAP6–GFP-expressing cells (A). Nuclei were stained with DAPI (blue). Insets show enlargements of the squares in merged photos. Scale bars: 10 μm, 1 μm (inset).

Journal of Cell Science (2015) 128, 1294–1307 doi:10.1242/jcs.155143

this ectopic localization to assess whether hSAXO1 can function to stabilize MTs *in vivo*. After exposure to 4℃, only cells expressing hSAXO1–GFP displayed a stabilized MT network, as observed in cells expressing MAP6–GFP. In cells expressing low amounts of hSAXO1–GFP (barely detectable, see Fig. 5B, 4℃), stabilization of interphase MTs upon cold treatment also occurred, which suggests that hSAXO1 can stabilize MTs against cold depolymerization and that a very small amount of the protein is needed for this to stabilization to occur.

In order to further characterize the domains in hSAXO1 that are responsible for MT targeting, binding and stabilization, we expressed truncated forms of hSAXO1–GFP and used immunodetection to examine their localization (detailed in Fig. 1C). Deletion of the last Mn repeat and C-terminal domain (Δ-Mn12-Cter–GFP) or of the C-terminal domain alone (Δ-Cter–GFP) did not modify either the centriolar localization of the protein or MT stabilization (Fig. 5D; supplementary material Fig. S3A). Furthermore, the N-terminal domain seems to be important for specific centriole localization, because constructs without the N-terminal domain (Δ-Nter–GFP, Mn1-12–GFP) bind to the MT network, at 37℃ and 4℃, without showing centriole specificity (Fig. 5E,G); however, the Nter–GFP protein localized throughout the cytoplasm and did not stabilize microtubules (Fig. 5F), suggesting that the N-terminal domain is sufficient for neither MT binding nor for centriole targeting, but might play a role in centriole retention. All truncations containing the Mn modules [Δ-Mn12-Cter–GFP, Δ-Nter–GFP, Mn1-12–GFP (Fig. 5D,E,G) and Δ-Cter–GFP (supplementary material Fig. S3A)] were able to bind to and cold-stabilize MTs, whereas the absence of these modules abolished it (Nter–GFP in Fig. 5F; and Nter+Cter–GFP in supplementary material Fig. S3A).

Two Mn modules (Mn1-2) are sufficient to bind to and stabilize MTs *in vitro* and *in vivo*

We wanted to address the MT-binding properties of hSAXO1 to MTs; thus, we used co-sedimentation assays. Because full-length hSAXO1 could not be produced as a soluble protein, we performed these experiments using soluble histidine-tagged truncated forms of the protein corresponding to the first 2 ($_{6His}$Mn1-2) and 3 ($_{6His}$Mn1-3) Mn modules (amino acids 30–97 and 30–131, respectively). $_{6His}$Mn1-2 and $_{6His}$Mn1-3 proteins were incubated with taxol-stabilized MTs at 37℃, then centrifuged to separate the pellet of microtubules and associated protein from the supernatant containing unbound protein. Equal amounts of each fraction were analyzed by SDS-PAGE. As shown in Fig. 6A, $_{6His}$Mn1-2 and $_{6His}$Mn1-3 were recovered in supernatant fractions when incubated alone (lanes 5b–7b and 11b–13b). Incubating increasing amounts of these proteins (0.6 µM, 2.3 µM and 11.7 µM) with MTs (7.2 µM tubulin) induced their sedimentation in the pellet fractions (lanes 2a–4a, 8a–10a), showing that $_{6His}$Mn1-2 or $_{6His}$Mn1-3 proteins bind directly to and sediment with MTs. Densitometric analysis showed that the percentage of these proteins found in the pellet fractions decreased with protein concentration, suggesting a critical concentration at which MTs became saturated and $_{6His}$Mn1-2 or $_{6His}$Mn1-3 was found in the supernatant fractions (Fig. 6B). Furthermore, at the lowest concentration tested (0.6 µM), most (93%) of the $_{6His}$Mn1-3 protein was recovered in the pellet fraction, whereas only half (46.1%) of $_{6His}$Mn1-2 protein co-sedimented, suggesting that $_{6His}$Mn1-3 has a higher affinity for MTs than $_{6His}$Mn1-2.

Mn modules have been described to stabilize MTs against cold-induced depolymerization (Bosc et al., 2001). To test whether the modules identified in hSAXO1 are indeed bona fide Mn modules, we performed an *in vitro* cold stabilization assay. MTs were mixed with $_{6His}$Mn1-2 or $_{6His}$Mn1-3 as described above, and incubated for 45 min on ice to induce MT depolymerization. The mixture was then centrifuged at 4℃, and pellet and supernatant fractions were analyzed by SDS-PAGE for the distribution of tubulin (Fig. 6C). When MTs alone are incubated at 37℃, the tubulin signal is recovered in the pellet fraction (lane 1a). Incubation of these MTs at 4℃ induces almost complete depolymerization, and the tubulin signal is then recovered in the supernatant fraction (compare tubulin signal in lanes 2a and 2b). However, the addition of $_{6His}$Mn1-3 and, to some extent, $_{6His}$Mn1-2 proteins prior to cold treatment prevented this cold-induced depolymerization in a dose-dependent manner. Gel densitometry and quantification show the percentage of stabilized MTs (polymerized tubulin) (ratio of tubulin signal in the pellet:total tubulin) with increasing concentration of $_{6His}$Mn1-2 and $_{6His}$Mn1-3 (Fig. 6D). Complete MT stabilization was observed with 2.3 µM of $_{6His}$Mn1-3 (1:3 protein:tubulin molar ratio), whereas $_{6His}$Mn1-2 did not fully stabilize MTs at the highest concentration tested (11.7 µM, 3:2 protein:tubulin molar ratio). The difference in binding between both constructs and their ability to cold-stabilize MTs suggests that MT-binding and stabilization of hSAXO1 depends on the number of Mn modules.

The Mn modules are required for MT binding and stabilization, with the first two being sufficient. We thus asked the question are the twelve modules (Mn1-12) required *in vivo*? To answer the question, we expressed Mn1-2–GFP, Mn1-3–GFP and Mn1-12–GFP in U-2OS cells (Fig. 6E). For Mn1-2–GFP and Mn1-3–GFP, non-extracted cells displayed high levels of cytoplasmic GFP labeling, masking potential MT labeling (data not shown). Detergent extraction before cell fixation followed by immunofluorescence showed that Mn1-12–GFP, Mn1-3–GFP and, to some extent, Mn1-2–GFP, did indeed bind to MTs at 37℃ and after incubation at 4℃ (Fig. 6E). To compare the MT-binding ability of the ectopic proteins, we quantified the percentage of transfected cells that retained GFP-decorated MTs after extraction compared to non-extracted cell samples (Fig. 6F). At 37℃ and 4℃, this showed an increase in the number of cells that retained GFP-decorated MTs together with an increasing number of Mn modules. Interestingly, for Mn1-3 (and Mn1-2 to some extent), incubation at 4℃ before extraction increased by more than twofold the percentage of cells that retained GFP-decorated MTs, thus suggesting either a temperature-induced increase in affinity or a temperature-related relocalization of the protein to the MTs. This temperature-related event could not be observed with Mn1-12, as all transfected cells already retained GFP-decorated MTs at 37℃.

hSAXO1 is involved in cilium length regulation

In an attempt to identify a centriole, basal body or axoneme-targeting domain, the localization of MAP6–GFP, hSAXO1–GFP and hSAXO1–GFP truncations was analyzed in transfected RPE1 cells incubated in low-serum medium for 24 h to induce ciliogenesis (Fig. 7). We show that MAP6–GFP localized throughout the cytoplasm, but also, that it localized in the primary cilium without specific basal body labeling (Fig. 7Ab). In contrast, and in accordance with the basal body and cilium localization of hSAXO1 (Fig. 4B), hSAXO1–GFP was observed specifically at the basal body, as well as along the axoneme of the primary cilium up to its distal tip (Fig. 7Ac). Basal body and

Journal of Cell Science (2015) 128, 1294–1307 doi:10.1242/jcs.155143

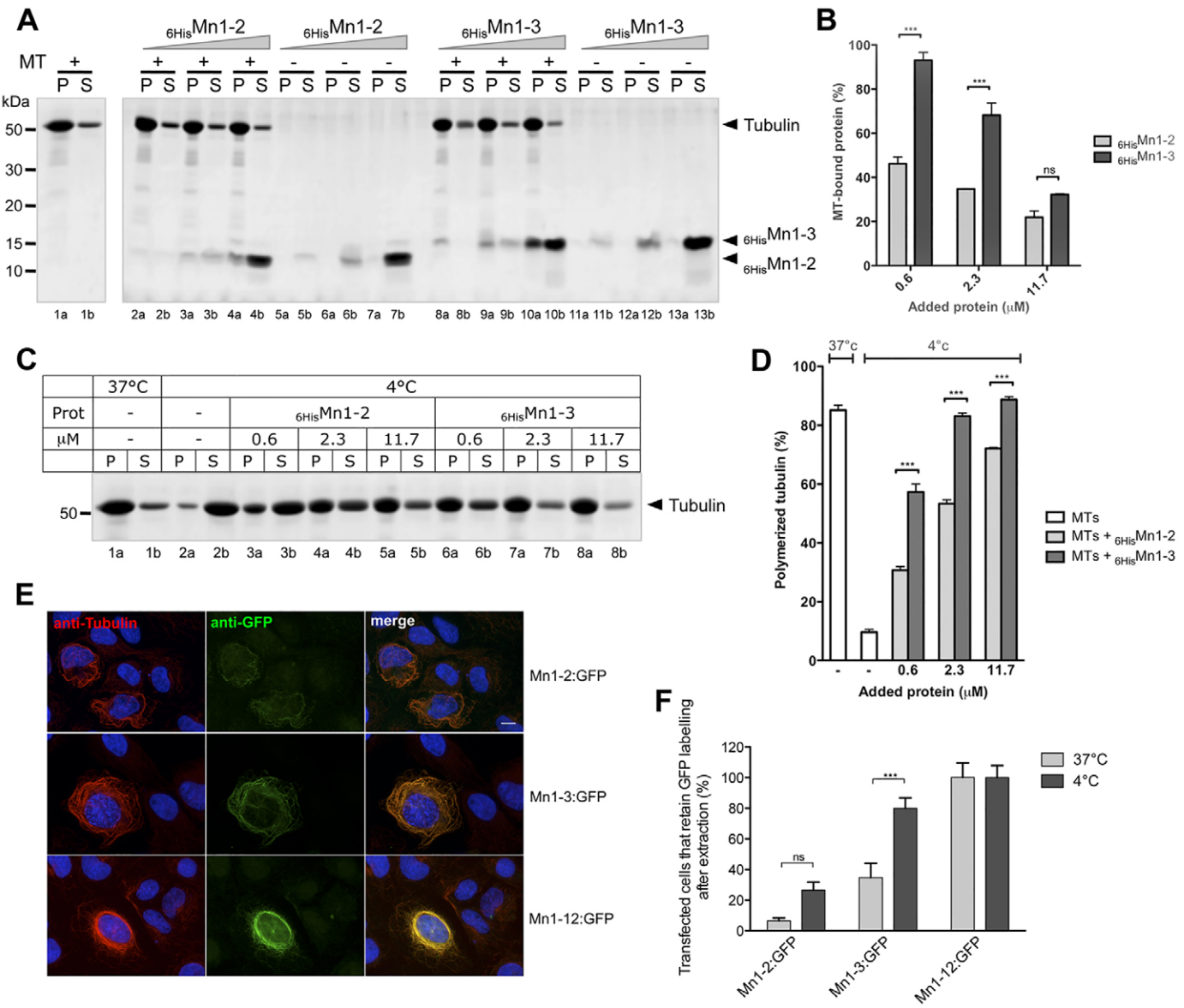

Fig. 6. Two Mn modules are sufficient for MT binding and stabilization both *in vitro* and *in vivo*. (A) Polymerized microtubules (7.2 μM tubulin) were incubated at 37°C with increasing concentrations of $_{6His}$Mn1-2 or $_{6His}$Mn1-3 proteins (0.6 μM, 2.3 μM and 11.7 μM), then pelleted by centrifugation. Pellet (P) and supernatant (S) samples were separated on a 12% SDS-PAGE gel. Gels were stained using Instant Blue (Expedeon). (B) Gels were analyzed by densitometry to quantify $_{6His}$Mn1-2 and $_{6His}$Mn1-3 proteins bound to MT (7.2 μM tubulin) at 37°C. (C) Polymerized microtubules (7.2 μM tubulin) were mixed at 37°C with increasing concentrations of recombinant proteins, then incubated at 4°C for 45 min before centrifugation. Pellet and supernatant samples were separated on a 12% SDS-PAGE gel. (D) Quantification of the MTs resistant to cold-induced depolymerisation. Gels from C were analyzed by densitometry to quantify the amount of polymerized tubulin remaining after cold treatment (45 min at 4°C) when incubated with buffer (MTs) or with the recombinant proteins (MTs+$_{6His}$Mn1-2 and MTs+$_{6His}$Mn1-3), and then cold-treated. (E) Anti-tubulin (red) and anti-GFP (green) immunolabeling of U-2OS cells expressing GFP-tagged (Mn1-2:GFP), Mn1-3 (Mn1-3:GFP) or Mn1-12 (Mn1-12:GFP) after 4°C incubation and Triton X-100 extraction. Scale bar: 10 μm. (F) Quantification of transfected cells that retain GFP labeling after extraction of cells incubated at 37°C or 4°C. Quantitative data show the mean±s.e.m.; ns, not significant; ***$P<0.001$.

cilium targeting of hSAXO1–GFP did not depend on the RVDP motif, as expression of the mutated form (R_{116}VDP→AADA) did not modify protein localization (data not shown). Nter–GFP (Fig. 7Ae) and Cter–GFP (data not shown) constructs localized throughout the cytoplasm and were not detected in the primary cilium, thus suggesting that the Mn domains are necessary for primary cilium localization. Indeed, specific axoneme-only localization was observed for Mn1-12–GFP, demonstrating that the Mn modules are required and sufficient for cilium targeting (Fig. 7Ad).

Mean cilium length in mock-transfected cells (3.4±0.06 μm; ±s.e.m) was in accordance with previous measurements (Kim et al., 2011). Mean cilium length in MAP6–GFP-expressing cells (4.0±0.1 μm) and Nter–GFP-expressing cells (3.2±0.3 μm) did not differ significantly from that of mock-transfected cells, suggesting that neither MAP6 nor the N-terminal domain of hSAXO1 influence primary cilium length (Fig. 7B). However, in hSAXO1–GFP- and Mn1-12–GFP-expressing cells, we observed a significant twofold increase in mean cilium length (6.5±0.2 μm and 6.9±0.3 μm, respectively) compared with that of mock-transfected

Journal of Cell Science (2015) 128, 1294–1307 doi:10.1242/jcs.155143

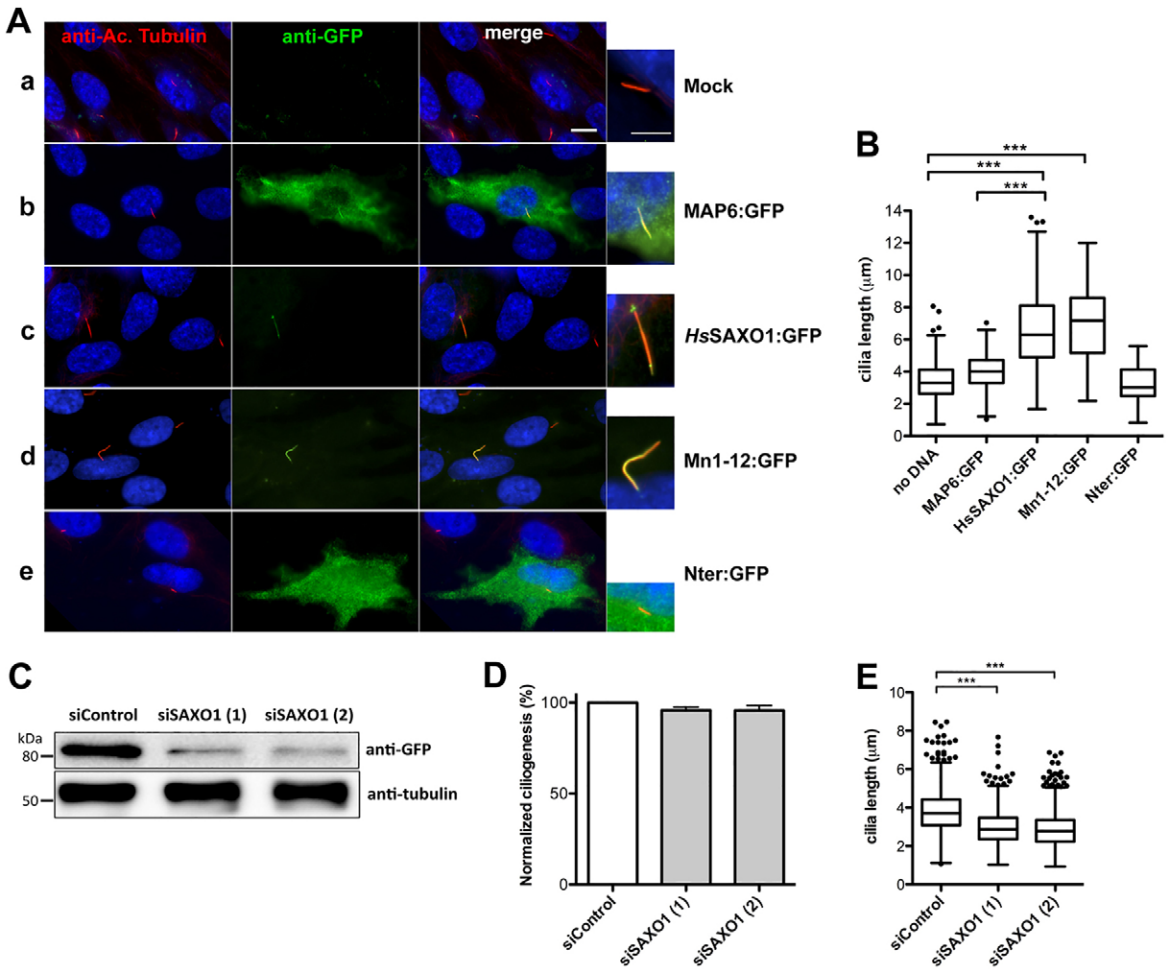

Fig. 7. Expression of truncated forms of hSAXO1 and siRNA-mediated knockdown identify a role for SAXO1 in determining cilium length. (A) Ectopic expression and localization of GFP-tagged MAP6 (MAP6:GFP) and truncations of GFP-tagged hSAXO1 (hSAXO1:GFP) in ciliated RPE1 cells. Transfected cells expressing the recombinant proteins were labeled with anti-acetylated (Ac.) tubulin (red) and anti-GFP (green). Scale bars: 10 μm, 5 μm (zoom images). (B) Tukey's box and whiskers plot of cilium length in RPE1 cells expressing the GFP-tagged constructs in A. Mean cilium length (±s.e.m.) was 3.40 μm±0.06 μm (mock-treated cells), 4.0±0.1 μm (MAP6–GFP), 3.2±0.3 μm (Nter–GFP), 6.5±0.2 μm (hSAXO1–GFP) and 6.9±0.3 μm (Mn1-12–GFP).*** $P<0.001$. (C) Western blot of U-2OS cells expressing hSAXO1–GFP and treated with siRNA for 48 h. Membranes were probed with anti-GFP (upper panel), stripped, then probed with anti-tubulin (lower panel). (D) The percentage of ciliated cells in siRNA-treated RPE1 cells. (E) Tukey's box and whiskers plot of cilium length in siRNA-treated RPE1 cells. Mean cilium length was 3.83±0.04 μm (siControl), 2.98±0.04 μm [siSAXO1(1)] and 2.90±0.03 μm [siSAXO1(2)]. ***$P<0.001$.

cells, suggesting a role of hSAXO1 in regulating axoneme length.

To further assess the roles of hSAXO1, we performed small interfering (si)RNA knockdown experiments. We treated cells with either control siRNA (siControl), hSAXO1-specific siRNAs [siSAXO1(1), siSAXO1(2)] or a pool of four siRNAs [siSAXO1(pool)]. As the endogenous level of hSAXO1 protein is not detectable by western blotting in these cells, and to control knockdown efficiency, we transfected U-2OS cells with the pcDNAhSAXO1-GFP vector 24 h before siRNA treatment and cells were processed for western blotting 48 h later. Western blot analysis using anti-GFP to detect the recombinant protein illustrated a decrease in hSAXO1–GFP signal in siSAXO1(1)- and in siSAXO1(2)-treated cells when compared with siControl-treated cells. After quantification and normalization to the tubulin loading control, we observed a decrease in hSAXO1–GFP of 81% [siSAXO1(1)] and 78% [siSAXO1(2)], demonstrating that siRNA knockdown was efficient (Fig. 7C). The decrease in hSAXO1–GFP expression was also observed in siSAXO1(pool)-treated cells (supplementary material Fig. S4A). U-2OS and RPE1 cells were then treated with siRNAs for 48 h and processed for immunofluorescence. hSAXO1 protein was still detected in both cell lines by immunofluorescence after siRNA treatments, suggesting its high stability as already shown for centriole proteins (Kochanski and Borisy, 1990). In U-2OS cells, siSAXO1 treatment did not affect centriole γ-tubulin labeling after either 37℃ or after 4℃ incubation, suggesting that centriole MTs were stable (data not shown). As the endogenous hSAXO1 was still detectable and very low amounts of proteins can stabilize microtubules (see the no or weak dotted labeling on U-2OS cells expressing hSAXO1–GFP with stabilized microtubules in Fig. 5), small amounts of residual protein could thus stabilize centriole MTs. In RPE1 cells, siSAXO1 treatment [with either of the two individual sequences (Fig. 7D) or the pool (supplementary material Fig. S4] did not affect the percentage of cells that formed cilia after 48 h of siRNA treatment, suggesting that the

protein is not involved in ciliogenesis per se. However, we observed a statistically significant decrease in mean cilium length in siSAXO1(1)- and in siSAXO1(2)-treated cells compared with that of siControl-treated cells after 24 h of ciliogenesis induction {mean cilium length of 2.98±0.04 µm [siSAXO1(1)] and 2.90±0.03 µm [siSAXO1(2)] compared to 3.83±0.04 µm (siControl); Fig. 7E}. The decrease in cilium length was also observed in siSAXO1(pool)-treated cells (supplementary material Fig. S4C), thus confirming the role of hSAXO1 in the regulation of cilium length.

DISCUSSION

MAP6 proteins (previously named STOP proteins) are vertebrate structural MAPs that stabilize MTs, upon cold or nocodazole treatment, through their Mc and Mn modules (Bosc et al., 1999; Bosc et al., 2003; Job et al., 1982). Recently, we identified the SAXO family of proteins (for stabilizer of axonemal microtubules) as MAP6-related proteins that are present only in flagellated or ciliated eukaryotes (Dacheux et al., 2012). As centrioles, basal bodies and axonemes all have stable MTs (Bettencourt-Dias and Glover, 2007), we suggest specific roles of the SAXO proteins in these structures that are parallel to the functions seen for MAP6 proteins in other MT subsets. In mammals, we identified two homologs, SAXO1 (FAM154A) and SAXO2 (FAM154B), and focused our study on hSAXO1. The existence of both MAP6 proteins in vertebrates and of two SAXO proteins in amniotes provides a framework to address diverging cellular requirements and to accommodate specific cellular functional requirements.

Our work demonstrates for the first time that hSAXO1 is a MAP6-related protein specific to centrioles and the MTs of related structures (basal bodies, primary cilia and the sperm axoneme). The results show that hSAXO1 is expressed in every human tissue and is predominantly expressed in testis, almost certainly as a consequence of its presence along the axoneme of the sperm flagellum. Endogenous hSAXO1 could be detected by western blotting in mature sperm but not in RPE1 and U-2OS cells. This is most probably owing to detection level limitations, as human sperm flagellum is positive for hSAXO1 along its full length, making it proportionally more abundant compared with its expression in other cell types. Basal body localization was also observed at the base of motile cilia of human bronchial epithelial cells; however, no signal could be detected in the axoneme. Interestingly, preliminary low-resolution immunohistochemistry work on tissue by the Swedish Human Protein Atlas (www.proteinatlas.org) demonstrated immunolabeling of hSAXO1 at the basal bodies of motile cilia of the fallopian tube, upper airway epithelia and epididymis epithelia, but showed that hSAXO2 is present in the axoneme aspect of these motile cilia (Uhlen et al., 2010). These data and our data suggest that, in motile cilia, hSAXO1 localizes only to basal bodies, except for the spermatozoa where it also localizes to the axoneme. hSAXO2 has not been identified in spermatozoa, suggesting complementary roles for these proteins and a fine regulation of localization and function in non-germinal cells.

We have shown here that overexpression of hSAXO1 in cultured cells conferred cold and drug stability to MTs, and *in vitro* and *in vivo* MT-binding and MT-stabilizing assays showed that the Mn modules are necessary and sufficient for direct MT binding and stabilization. MT binding is often mediated by repeated motifs (MAP1, 2, 4, 6 and 9, tau, doublecortin/DCLK, BPAG1) (Amos and Schlieper, 2005), and neuronal MAP6 has three functionally characterized Mn modules with the first two being sufficient for MT binding and stabilization (Bosc et al., 2001; Lefèvre et al., 2013). Our *in vitro* and *in vivo* studies demonstrate that increasing the number of Mn modules increases MT binding and stabilization, with two out of twelve Mn modules being sufficient, and that the N-terminal domain might play a role in retention at the centriole. Interestingly, out of six Mn modules, only four are required for correct *in vivo* localization of SPM1 (*Tg*SAXO) in *T. gondii*, and two are sufficient for MT-binding and stabilization (Tran et al., 2012), which is similar to MAP6 Mn1-Mn2 modules (Bosc et al., 2001).

Centriole, basal body and axoneme localization of hSAXO1 requires the Mn modules. But why does hSAXO1 localize specifically to the MTs of these structures and MAP6 does not? We can propose several hypotheses. First, hSAXO1 binding to centrioles and related structures could be specific to tubulin PTMs. It has been demonstrated that the glutamate lateral chain acts as a regulator for the binding of microtubule-associated proteins (MAPs) (Boucher et al., 1994) and that glutamylation is required for centriole stability (Bobinnec et al., 1998). Second, specific binding could be through the C-terminal tail of βI and βIV-tubulin isoforms that contain the 'axoneme EGEFXXX motif' present in most β tubulins that are expressed in ciliated or flagellated tissues or organisms (Dutcher, 2001; Jensen-Smith et al., 2003; Nielsen et al., 2001). Third, the specificity could be due to the hSAXO1 cysteine-rich N-terminal domain that might serve as a retention signal. Despite N-terminal sequence differences between hSAXO1 and MAP6, it is striking that N-terminal cysteine clusters are conserved in all proteins. This could confer N-terminal palmitoylation and membrane interaction to some hSAXO1 variants. Indeed, cilium targeting of several proteins depends on such PTMs (Hsiao et al., 2012), and the cysteine-rich N-terminal domain of MAP6 can be palmitoylated to allow Golgi targeting (Gory-Fauré et al., 2006). This suggests that N-terminal PTM of hSAXO1 could be involved in centriole retention or release towards the axoneme to regulate axoneme building and stability.

In mammalian sperm, an ATP-independent MT cold-stabilizing factor other than MAP6 was identified, but not at the molecular level (Eyer et al., 1990). From our data, we can propose that SAXO1 could be this cold-stabilizing factor. Interestingly, calmodulin kinase II (CaMKII) might regulate sperm flagellum motility (Schlingmann et al., 2007). CaMKII phosphorylates MAP6, promoting its relocalization from MTs to actin assemblies (Baratier et al., 2006). The CaMKII/actin relationship of MAP6 can thus be elaborated for SAXO1, as our unpublished data show that tSAXO interacts with *Tb*Actin in a yeast two-hybrid assay and that tSAXO also targets specifically to the primary cilium when expressed in RPE1 cells (supplementary material Fig. S3B). MAP6 has been proposed to play a role as a temperature sensor (Delphin et al., 2012). One can speculate that CaMKII, in response to temperature variations, modulates the MT interaction of SAXO1 in sperm, which, in turn, would regulate axoneme function. Indeed, *Mus musculus* (*Mm*)SAXO1 Ser449 is phosphorylated within a CaMKII (R/K-X-X-S/T) consensus sequence (Platt et al., 2009); however, the role of this phosphorylation has yet to be determined.

We have shown that overexpression of MAP6 in RPE1 cells (in which MAP6 localizes throughout the cell, including at the primary cilium) does not interfere with cilium length, whereas modulation of hSAXO1 expression (which localizes specifically to the primary cilium), by overexpression or knockdown, influences cilium length, thus suggesting a role in the construction of or biogenesis

of these axonemes. Marshall and colleagues have proposed the 'balance-point model' of cilium length control, where axoneme length is regulated by the intraflagellar-transport-dependent rates of assembly and disassembly of tubulin (Marshall et al., 2005; Marshall and Rosenbaum, 2001). In light of this model, we propose here that overexpression of hSAXO1 would increase the stability of the axoneme MTs and, as a consequence, the disassembly rate of tubulin would decrease, with the assembly rate not being modified, thus shifting the length set-point to a longer length. In contrast, knockdown of hSAXO1 would reduce the MT stability of the growing axoneme, thus shifting the length set-point to a shorter length. It was demonstrated recently that the ubiquitously expressed MAP4 is present in the flagellum of human sperm (Baker et al., 2013), and is also a component of the primary cilium, playing an antagonistic role to control axonemal microtubule growth (Ghossoub et al., 2013). The presence of several MAPs in cilia, such as MAP4 and SAXO1, could thus participate in the fine regulation of axoneme length.

From our data, we can propose several roles for hSAXO1 in cilia and related structures, and these depend on the cell type in which the protein is expressed. First, hSAXO1 is a MT-stabilizing protein localizing specifically at the most stable MT-based structures and thus could be one of the major stabilizing factors of centrioles, basal bodies and axoneme MTs. Second, considering that hSAXO1 is involved in the regulation of primary cilium axoneme length, it could act as a component of the axoneme length control machinery (Miyoshi et al., 2011). hSAXO1 could thus be a key player in the biogenesis, stability and length of the sperm flagellum.

Clearly, more detailed analysis of these protein families will be required to gain additional data on the respective specificities of MAP6 and SAXO proteins in the binding and stabilization of MTs. Such data could open new exciting avenues for the potential roles of the SAXO proteins in human physiology and in pathologies such as ciliopathies and infertility.

MATERIALS AND METHODS

In silico analysis, sequence database analysis and statistics

SAXO orthologs were identified by walking BLASTP as in Dacheux et al. (Dacheux et al., 2012). The human *FAM154A* sequence (NM_153707.2) was used to screen human genomic, EST and cDNA databases with the BLAST program. Matching ESTs were then analyzed for their exon content, and the identified exons were reported into the gene sequence. Accession numbers for protein sequences are listed in supplementary material Table S2. MEME analysis (Bailey et al., 2006) settings were: any number of repetitions, 4 different motifs with a minimum width of 6 and a maximum width of 50. MEME analysis settings for the Mn12-Cter sequences were: any number of repetitions, 1 motif with a minimum width of 6 and a maximum width of 10. For cilium length measurements in overexpression experiments, statistical analyses were performed with Prism software (GraphPad, Inc.) using analysis of variance (ANOVA) followed by Bonferroni's multiple comparison test using data from three independent experiments. Student's *t*-tests followed by Fischer's tests were used for ciliogenesis and cilium length measurements in siRNA experiments. In Tukey's box and whiskers plots of cilia length, boxes represent the two central quartiles (50% of data points) with the inside bar being the median. Whiskers represent the highest and lowest data points in the 1.5 interquartile range (Tukey's boxplot). Data are plotted as the mean±s.e.m.

Cell lines, growth conditions and transfection

U-2OS (Heldin et al., 1986) cells were grown as in Dacheux et al. (Dacheux et al., 2012). hTERT-RPE1 (RPE1) cells (Jiang et al., 1999) were grown as in Ghossoub et al. (Ghossoub et al., 2013). To induce ciliogenesis, confluent RPE1 cells were incubated in low-serum medium (0.5% FCS) for 24 h. Cells were transfected using Lipofectamine 2000 (Invitrogen) and processed for immunofluorescence as in Dacheux et al. (Dacheux et al., 2012). For MT stabilization assays after cold exposure or nocodazole treatment, cells were incubated for 45 min at 4℃ or with 20 µM nocodazole at 37℃ prior to immunofluorescence. HBECS were obtained from the Centre Hospitalier Universitaire (CHU) of Bordeaux, France, with approval from the local ethics committee, and were differentiated as described previously (Gras et al., 2012). Knockdown experiments used a non-targeting control siRNA pool (ON-TARGETplus-Non-targeting pool, Dharmacon) and a hSAXO1 siRNA targeting pool (ON-TARGETplus-SMART pool, Dharmacon) or individual sequences [ON-TARGETplus-FAM154A siRNA siSAXO1(1) and siSAXO1(2)] (supplementary material Table S3). siRNAs (20 nM final concentration) were delivered into cells by transfection using Lipofectamine RNAiMax (Invitrogen) (1 µl/well in 24-well plates or 3 µl/well in six-well plates) according to the manufacturer's instructions. Transient transfection of plasmids (1 µg/well in 24-well plates or 3 µg/well in six-well plates) was performed using Lipofectamine 2000 (Invitrogen). RPE1 and U-2OS cells were plated and transfected on the second day with siRNAs (or plasmids) and the third day with plasmids (or siRNA) then grown for 24 h or 48 h prior to analysis. Ciliogenesis in RPE1 cells was induced with 0.5% FCS medium at 24 h post-transfection for another 24 h.

Sperm preparation

Human sperm collection was conducted in accordance with hospital ethical guidelines (authorisation DC-2011-1381). Normal ejaculated semen samples were washed in 10 ml of PBS (800 ***g***, 10 min) and used for further steps or stored in 10% DMSO in PBS at −80℃.

Antibodies

Primary antibodies were: anti-hSAXO1 (raised against the last 94 amino acids of the protein; Atlas antibodies HPA023899; immunofluorescence 1:25–50, western blotting 1:500), anti-acetylated tubulin (Sigma T7451; immunofluorescence 1:1000), anti-γ-tubulin (Sigma T-5326; immunofluorescence 1:1000), anti-pericentrin (Abcam Ab28144; immunofluorescence 1:50), anti-α-tubulin (Sigma T9026; immunofluorescence 1:500) and TAT1 (Woods et al., 1989; immunofluorescence 1:100, western blotting 1:1000, kind gift from Keith Gull, University of Oxford, UK), anti-GFP (Clontech 632460; immunofluorescence, western blotting 1:1000). Secondary antibodies used for western blotting or immunofluorescence were: horseradish peroxidase (HRP)-conjugated anti-rabbit-IgG (Sigma A-9169; 1:10,000), HRP-conjugated anti-mouse+IgM (Jackson, 115-035-044; 1:10,000), FITC-conjugated anti-rabbit-IgG (Sigma F-0511; 1:200), Alexa-Fluor-647-conjugated anti-mouse-IgG (Invitrogen A-21235; 1:400).

Immunofluorescence

Except for the γ-tubulin and pericentrin immunolabeling, sperm and HBECs samples were fixed in −20℃ methanol, and U-2OS and RPE1 cells were fixed in 3% paraformaldehyde (PFA) in PBS for 15 min at 37℃. After PFA neutralization in 100 mM glycine for 10 min, cells were washed twice in PBS. HBEC samples were fixed after 21 days of differentiation. For cytoskeleton-extracted cell experiments, transfected U-2OS cells were extracted, PFA fixed, permeabilized and incubated with primary then secondary antibodies as in Dacheux et al. (Dacheux et al., 2012). Aliquots of semen samples were permeabilized, washed in PBS, spread on poly-L-lysine-coated glass slides, dried overnight, rehydrated in PBS, fixed at −20℃ for 1 h in methanol, washed in PBS, incubated with primary antibodies then secondary antibodies and DAPI stained as in Dacheux et al. (Dacheux et al., 2012). The slides were mounted in Prolong (Invitrogen).

Images were acquired on a Zeiss Imager-Z1 microscope with a 100× or 63× (NA1.4) objectives with Metamorph® software (Molecular Devices), using a Photometrics Coolsnap HQ2 camera, and processed with ImageJ. All images were digitally acquired under identical instrument settings within a set of experiments. Cilium length was

measured using ImageJ64. Measurements were performed on three independent experiments with $n=361$, $n=110$, $n=178$, $n=77$ and $n=18$ for Mock, MAP6–GFP, hSAXO1–GFP, Mn1-12–GFP and Nter–GFP overexpression experiments, respectively, and with $n=592$ (siControl), $n=510$ [siSAXO1(1)], and $n=624$ [siSAXO1(2)] for the cilium length in siRNA experiments.

Western blotting

Proteins (20 µg) were separated on a 12% SDS-PAGE gel, transferred onto PVDF membranes and probed with primary and secondary antibodies as in Dacheux et al. (Dacheux et al., 2012), followed by detection with the Biorad Clarity-ECL kit (170-5061). Western blots were quantified using ImageJ, and hSAXO1–GFP levels were normalized based on the tubulin loading controls.

RT-PCR and RT-qPCR

Semi-quantitative RT-PCR was performed on human total RNA master panel (FirstChoice, AM6000) and on human total RNA of fallopian tube (Agilent Technologies, #540057) with a primer pair common to isoforms 1, 2 and 3 that amplified a 296-bp fragment corresponding to part of exon 12. Human β-actin (BC002409) was used as a control for RNA integrity and was amplified with an internal control primer pair amplifying a 564-bp fragment (supplementary material Table S3). RT-qPCR was performed using the Promega GoTaq One-Step-RTqPCR kit in a CFX96 apparatus (BioRad C1000 TOUCH Thermal Cycler). Reactions were performed in duplicate in a total volume of 20 µl using 20 ng of total RNA from the different tissues as matrix. CT values for hSAXO1 were corrected for *GAPDH* and β2-microglobulin signals in corresponding tissues. hSAXO1 expression levels were then expressed relative to the strongest expressing human tissue (testis).

Plasmids

The MAP6–GFP-expressing vector encodes a GFP-tagged MAP6-N isoform (kind gift from Christian Delphin, Institut des Neurosciences, Grenoble, France). The hSAXO1 (*FAM154A*) ORF from the RC206724 vector (Origene) and truncations were amplified by PCR and subcloned into pcDNA3.1/CT-GFP TOPO (Invitrogen). Mutation of the putative cilium targeting sequence (R_{116}VDP→AADA) was performed by site-directed mutagenesis (Stratagene QuikChange Site-directed mutagenesis kit).

The hSAXO1-*Mn1-12* sequence (corresponding to amino acids 30–434) was cloned into the pET28a (+) in frame with a N-terminal 6×histidine tag. pET28a-hSAXO1 *Mn1-2* (amino acids 30–97) and pET28a-hSAXO1-*Mn1-3* (amino acids 30–131) were obtained by introducing a stop codon after Mn2 or Mn3 in the pET28a-hSAXO1 *Mn1-12* plasmid by site-directed mutagenesis. All DNA sequences were checked by DNA sequencing.

$_{6His}$Mn1-2 and $_{6His}$Mn1-3 expression and purification

Protein expression was induced in BL21(*DE3*) bacteria with 1 mM IPTG and purified as follows. Induced cells (500 ml, 2 h induction) were pelleted and resuspended in 25 ml of buffer [50 mM sodium phosphate pH 7.5, 200 mM NaCl, 1 mM DTT, protease inhibitors (Calbiochem Cocktail III), 0.1 mg/ml lysozyme]. Cells were sonicated on ice and centrifuged at 10,000 ***g*** for 20 min at 4℃. The supernatant was loaded on a 1-ml HisTrap™ FF column (GE Healthcare) and the protein was eluted with a 20-ml gradient of 70–500 mM imidazole. Prior to co-sedimentation assays, proteins were dialyzed overnight against 1000× volumes of fresh PEMD buffer (100 mM PIPES pH 6.8, 1 mM EGTA, 1 mM $MgCl_2$, 1 mM DTT) at 4℃. After dialysis, proteins were centrifuged for 10 min at 21,000 ***g*** and protein concentration was determined using the Pierce-660 Protein Assay kit. Proteins were diluted to equal molar concentrations in PEMD.

Co-sedimentation assays

Taxol-stabilized MTs (5 mg/ml) were prepared as follows based on a method published previously (Campbell and Slep, 2011). Purified bovine tubulin (>99% pure, Cytoskeleton Inc.) was resuspended in cold G-PEM (80 mM PIPES pH 6.8, 1 mM EGTA, 0.5 mM $MgCl_2$, 1 mM GTP) and centrifuged at 4℃ for 10 min at 16,000 ***g*** to remove aggregated protein. Taxol (Paclitaxel, Calbiochem®) was added stepwise (addition of 1/10 of the final volume of 5 µM, 50 µM and 500 µM taxol in DMSO, with a 10-min incubation at 37℃ after each addition) to reach a final concentration of 5 mg/ml tubulin MT preparation. For co-sedimentation assays, 4 µl of MTs were mixed with different amounts of protein. Volumes were adjusted to 50 µl with PEMD (7.2 µM tubulin final concentration). Samples were then incubated for 45 min at 37℃ or 4℃ and centrifuged for 15 min at 16,000 ***g*** at the corresponding temperature. Supernatants and pellets were separated and brought to equal volumes in SDS sample buffer and analyzed by SDS-PAGE. Gels were stained using Instant Blue™ (Expedeon) and analyzed by quantitative densitometry (ImageScanner, Amersham-Pharmacia Biotech).

Immunoelectron microscopy

Sperm aliquots were washed in PBS. Cells were resuspended in 50 mM sodium borate pH 9, 1% Triton X-100 and 2 mM DTT for 40 min at 4℃, and washed in PBS. Cells were placed on Parafilm and poly-L-Lysine pre-treated Butvar-coated G200 grids (EMS) and were floated onto the droplet for 10 min. Cells were fixed with 2% PFA in PBS (10 min), neutralized with 100 mM glycine in PBS (twice, for 10 min each), blocked in 0.1% BSA, 0.1% Tween-20 in PBS for 5 min, then transferred to a 50-µl droplet of anti-hSAXO1 (1:50 in blocking buffer) or anti-tubulin (TAT1, neat) at 4℃ overnight. Grids were blocked and incubated on 50-µl droplets of a 50/50 mixture of 6-nm (hSAXO1) or 10-nm (tubulin) Protein-A- and Protein-G-coated gold particles (Aurion), 1:20 in blocking buffer at 4℃ overnight. Grids were washed in blocking buffer, and then subjected to four 10-min washes in 0.01% BSA, 0.01% Tween-20 in PBS, and PBS. Sperm were post-fixed (1% glutaraldehyde, 30 min), washed four times for 10 min each in water, then negatively stained with 2× 10 µl in a 50/50 mixture of NanoVan/NanoW (2011, 2018, Nanoprobes). Grids were visualized on a FEI-Tecnai-12 electron microscope.

Acknowledgements

We thank Delphin (U836) for the MAP6–GFP vector, Gull (University of Oxford) for the TAT1 antibody, Lambert (UMR5248) for access to the ImageScanner, Chalard, Marcos and Cougnet-Houlery (UMR5234) for the continued lab infrastructure and Benmerah (INSERM U1163) and Byard (University of Winnipeg) for critical reading of the manuscript.

Competing interests

The authors declare no competing or financial interests.

Author contributions

D.D., B.R. and M.B. conceived of the project and designed experiments. D.D., B.R., N.L., E.R., L.C., T.T., A.P.R., R.M., D.R.R. and M.B. performed and analyzed experiments. C.B. and A.A. performed gene analysis. L.C., T.T., A.P.-R. and R.M. analyzed experiments on human samples. M.B. wrote the manuscript with input of all authors.

Funding

This work was funded by a Projet Exploratoire Premier Soutien from the Centre National de la Recherche Scientifique to M.B., the Structure Fédérative de Recherche TransBioMed to M.B., the Agence Nationale de la Recherche [grant number ANR-09-BLAN0074 to M.B. and D.R.R.], Région Aquitaine grant [grant number 2011-13-01-014 to D.R.R.].

Supplementary material

Supplementary material available online at
http://jcs.biologists.org/lookup/suppl/doi:10.1242/jcs.155143/-/DC1

References

Amos, L. A. and Schlieper, D. (2005). Microtubules and maps. *Adv. Protein Chem.* **71**, 257-298.

Andrieux, A., Salin, P. A., Vernet, M., Kujala, P., Baratier, J., Gory-Fauré, S., Bosc, C., Pointu, H., Proietto, D., Schweitzer, A. et al. (2002). The suppression of brain cold-stable microtubules in mice induces synaptic defects associated with neuroleptic-sensitive behavioral disorders. *Genes Dev.* **16**, 2350-2364.

Arama, J., Boulay, A. C., Bosc, C., Delphin, C., Loew, D., Rostaing, P., Amigou, E., Ezan, P., Wingertsmann, L., Guillaud, L. et al. (2012). Bmcc1s, a novel brain-isoform of Bmcc1, affects cell morphology by regulating MAP6/STOP functions. *PLoS ONE* **7**, e35488.
Bailey, T. L., Williams, N., Misleh, C. and Li, W. W. (2006). MEME: discovering and analyzing DNA and protein sequence motifs. *Nucleic Acids Res.* **34**, W369-W373.
Baker, M. A., Hetherington, L., Reeves, G., Müller, J. and Aitken, R. J. (2008a). The rat sperm proteome characterized via IPG strip prefractionation and LC-MS/MS identification. *Proteomics* **8**, 2312-2321.
Baker, M. A., Hetherington, L., Reeves, G. M. and Aitken, R. J. (2008b). The mouse sperm proteome characterized via IPG strip prefractionation and LC-MS/MS identification. *Proteomics* **8**, 1720-1730.
Baker, M. A., Naumovski, N., Hetherington, L., Weinberg, A., Velkov, T. and Aitken, R. J. (2013). Head and flagella subcompartmental proteomic analysis of human spermatozoa. *Proteomics* **13**, 61-74.
Baratier, J., Peris, L., Brocard, J., Gory-Fauré, S., Dufour, F., Bosc, C., Fourest-Lieuvin, A., Blanchoin, L., Salin, P., Job, D. et al. (2006). Phosphorylation of microtubule-associated protein STOP by calmodulin kinase II. *J. Biol. Chem.* **281**, 19561-19569.
Behnke, O. and Forer, A. (1967). Evidence for four classes of microtubules in individual cells. *J. Cell Sci.* **2**, 169-192.
Bettencourt-Dias, M. and Glover, D. M. (2007). Centrosome biogenesis and function: centrosomics brings new understanding. *Nat. Rev. Mol. Cell Biol.* **8**, 451-463.
Bobinnec, Y., Khodjakov, A., Mir, L. M., Rieder, C. L., Eddé, B. and Bornens, M. (1998). Centriole disassembly in vivo and its effect on centrosome structure and function in vertebrate cells. *J. Cell Biol.* **143**, 1575-1589.
Bornens, M. (2002). Centrosome composition and microtubule anchoring mechanisms. *Curr. Opin. Cell Biol.* **14**, 25-34.
Bosc, C., Oenarier, E., Andrieux, A. and Job, D. (1999). STOP proteins. *Cell Struct. Funct.* **24**, 393-399.
Bosc, C., Frank, R., Denarier, E., Ronjat, M., Schweitzer, A., Wehland, J. and Job, D. (2001). Identification of novel bifunctional calmodulin-binding and microtubule-stabilizing motifs in STOP proteins. *J. Biol. Chem.* **276**, 30904-30913.
Bosc, C., Andrieux, A. and Job, D. (2003). STOP proteins. *Biochemistry* **42**, 12125-12132.
Boucher, D., Larcher, J. C., Gros, F. and Denoulet, P. (1994). Polyglutamylation of tubulin as a progressive regulator of in vitro interactions between the microtubule-associated protein Tau and tubulin. *Biochemistry* **33**, 12471-12477.
Brinkley, B. R. and Cartwright, J., Jr (1975). Cold-labile and cold-stable microtubules in the mitotic spindle of mammalian cells. *Ann. N. Y. Acad. Sci.* **253**, 428-439.
Campbell, J. N. and Slep, K. C. (2011). αβ-Tubulin and microtubule-binding assays. *Methods Mol. Biol.* **777**, 87-97.
Carvalho-Santos, Z., Azimzadeh, J., Pereira-Leal, J. B. and Bettencourt-Dias, M. (2011). Evolution: tracing the origins of centrioles, cilia, and flagella. *J. Cell Biol.* **194**, 165-175.
Dacheux, D., Landrein, N., Thonnus, M., Gilbert, G., Sahin, A., Wodrich, H., Robinson, D. R. and Bonhivers, M. (2012). A MAP6-related protein is present in protozoa and is involved in flagellum motility. *PLoS ONE* **7**, e31344.
Debec, A., Sullivan, W. and Bettencourt-Dias, M. (2010). Centrioles: active players or passengers during mitosis? *Cell. Mol. Life Sci.* **67**, 2173-2194.
Delphin, C., Bouvier, D., Seggio, M., Couriol, E., Saoudi, Y., Denarier, E., Bosc, C., Valiron, O., Bisbal, M., Arnal, I. et al. (2012). MAP6-F is a temperature sensor that directly binds to and protects microtubules from cold-induced depolymerization. *J. Biol. Chem.* **287**, 35127-35138.
Denarier, E., Fourest-Lieuvin, A., Bosc, C., Pirollet, F., Chapel, A., Margolis, R. L. and Job, D. (1998). Nonneuronal isoforms of STOP protein are responsible for microtubule cold stability in mammalian fibroblasts. *Proc. Natl. Acad. Sci. USA* **95**, 6055-6060.
Dinkel, H., Michael, S., Weatheritt, R. J., Davey, N. E., Van Roey, K., Altenberg, B., Toedt, G., Uyar, B., Seiler, M., Budd, A. et al. (2012). ELM – the database of eukaryotic linear motifs. *Nucleic Acids Res.* **40**, D242-D251.
Dinkel, H., Van Roey, K., Michael, S., Davey, N. E., Weatheritt, R. J., Born, D., Speck, T., Krüger, D., Grebnev, G., Kuban, M. et al. (2014). The eukaryotic linear motif resource ELM: 10 years and counting. *Nucleic Acids Res.* **42**, D259-D266.
Dorus, S., Busby, S. A., Gerike, U., Shabanowitz, J., Hunt, D. F. and Karr, T. L. (2006). Genomic and functional evolution of the Drosophila melanogaster sperm proteome. *Nat. Genet.* **38**, 1440-1445.
Dutcher, S. K. (2001). Motile organelles: the importance of specific tubulin isoforms. *Curr. Biol.* **11**, R419-R422.
Eyer, J., White, D. and Gagnon, C. (1990). Presence of a new microtubule cold-stabilizing factor in bull sperm dynein preparations. *Biochem. J.* **270**, 821-824.
Firat-Karalar, E. N., Sante, J., Elliott, S. and Stearns, T. (2014). Proteomic analysis of mammalian sperm cells identifies new components of the centrosome. *J. Cell Sci.* **127**, 4128-4133.
Fliegauf, M., Benzing, T. and Omran, H. (2007). When cilia go bad: cilia defects and ciliopathies. *Nat. Rev. Mol. Cell Biol.* **8**, 880-893.
Galiano, M. R., Bosc, C., Schweitzer, A., Andrieux, A., Job, D. and Hallak, M. E. (2004). Astrocytes and oligodendrocytes express different STOP protein isoforms. *J. Neurosci. Res.* **78**, 329-337.
Geng, L., Okuhara, D., Yu, Z., Tian, X., Cai, Y., Shibazaki, S. and Somlo, S. (2006). Polycystin-2 traffics to cilia independently of polycystin-1 by using an N-terminal RVxP motif. *J. Cell Sci.* **119**, 1383-1395.
Ghossoub, R., Hu, Q., Failler, M., Rouyez, M. C., Spitzbarth, B., Mostowy, S., Wolfrum, U., Saunier, S., Cossart, P., Jamesnelson, W. et al. (2013). Septins 2, 7 and 9 and MAP4 colocalize along the axoneme in the primary cilium and control ciliary length. *J. Cell Sci.* **126**, 2583-2594.
Gory-Fauré, S., Windscheid, V., Bosc, C., Peris, L., Proietto, D., Franck, R., Denarier, E., Job, D. and Andrieux, A. (2006). STOP-like protein 21 is a novel member of the STOP family, revealing a Golgi localization of STOP proteins. *J. Biol. Chem.* **281**, 28387-28396.
Gras, D., Bourdin, A., Vachier, I., de Senneville, L., Bonnans, C. and Chanez, P. (2012). An ex vivo model of severe asthma using reconstituted human bronchial epithelium. *J. Allergy Clin. Immunol.* **129**, 1259-1266.e1.
Grimes, G. W. and Gavin, R. H. (1987). Ciliary protein conservation during development in the ciliated protozoan, Oxytricha. *J. Cell Biol.* **105**, 2855-2859.
Guerrero, K., Monge, C., Brückner, A., Puurand, U., Kadaja, L., Käämbre, T., Seppet, E. and Saks, V. (2010). Study of possible interactions of tubulin, microtubular network, and STOP protein with mitochondria in muscle cells. *Mol. Cell. Biochem.* **337**, 239-249.
Heldin, C. H., Johnsson, A., Wennergren, S., Wernstedt, C., Betsholtz, C. and Westermark, B. (1986). A human osteosarcoma cell line secretes a growth factor structurally related to a homodimer of PDGF A-chains. *Nature* **319**, 511-514.
Hesketh, J. E., Ciesielski-Treska, J. and Aunis, D. (1984). Cold-stable microtubules and microtubule-organizing centres in astrocytes in primary culture. *Neurosci. Lett.* **51**, 155-160.
Hinchcliffe, E. H. and Linck, R. W. (1998). Two proteins isolated from sea urchin sperm flagella: structural components common to the stable microtubules of axonemes and centrioles. *J. Cell Sci.* **111**, 585-595.
Hoh, R. A., Stowe, T. R., Turk, E. and Stearns, T. (2012). Transcriptional program of ciliated epithelial cells reveals new cilium and centrosome components and links to human disease. *PLoS ONE* **7**, e52166.
Hsiao, Y. C., Tuz, K. and Ferland, R. J. (2012). Trafficking in and to the primary cilium. *Cilia* **1**, 4.
Hu, H., Columbus, J., Zhang, Y., Wu, D., Lian, L., Yang, S., Goodwin, J., Luczak, C., Carter, M., Chen, L. et al. (2004). A map of WW domain family interactions. *Proteomics* **4**, 643-655.
Janke, C., Rogowski, K. and van Dijk, J. (2008). Polyglutamylation: a fine-regulator of protein function? 'Protein modifications: beyond the usual suspects' review series. *EMBO Rep.* **9**, 636-641.
Jenkins, P. M., Hurd, T. W., Zhang, L., McEwen, D. P., Brown, R. L., Margolis, B., Verhey, K. J. and Martens, J. R. (2006). Ciliary targeting of olfactory CNG channels requires the CNGB1b subunit and the kinesin-2 motor protein, KIF17. *Curr. Biol.* **16**, 1211-1216.
Jensen-Smith, H. C., Ludueña, R. F. and Hallworth, R. (2003). Requirement for the betaI and betaIV tubulin isotypes in mammalian cilia. *Cell Motil. Cytoskeleton* **55**, 213-220.
Jiang, X. R., Jimenez, G., Chang, E., Frolkis, M., Kusler, B., Sage, M., Beeche, M., Bodnar, A. G., Wahl, G. M., Tlsty, T. D. et al. (1999). Telomerase expression in human somatic cells does not induce changes associated with a transformed phenotype. *Nat. Genet.* **21**, 111-114.
Job, D., Rauch, C. T., Fischer, E. H. and Margolis, R. L. (1982). Recycling of cold-stable microtubules: evidence that cold stability is due to substoichiometric polymer blocks. *Biochemistry* **21**, 509-515.
Kim, S., Zaghloul, N. A., Bubenshchikova, E., Oh, E. C., Rankin, S., Katsanis, N., Obara, T. and Tsiokas, L. (2011). Nde1-mediated inhibition of ciliogenesis affects cell cycle re-entry. *Nat. Cell Biol.* **13**, 351-360.
Kochanski, R. S. and Borisy, G. G. (1990). Mode of centriole duplication and distribution. *J. Cell Biol.* **110**, 1599-1605.
Lefèvre, J., Savarin, P., Gans, P., Hamon, L., Clément, M. J., David, M. O., Bosc, C., Andrieux, A. and Curmi, P. A. (2013). Structural basis for the association of MAP6 protein with microtubules and its regulation by calmodulin. *J. Biol. Chem.* **288**, 24910-24922.
Lieuvin, A., Labbé, J. C., Dorée, M. and Job, D. (1994). Intrinsic microtubule stability in interphase cells. *J. Cell Biol.* **124**, 985-996.
Margolis, R. L., Rauch, C. T. and Job, D. (1986). Purification and assay of a 145-kDa protein (STOP145) with microtubule-stabilizing and motility behavior. *Proc. Natl. Acad. Sci. USA* **83**, 639-643.
Margolis, R. L., Rauch, C. T., Pirollet, F. and Job, D. (1990). Specific association of STOP protein with microtubules in vitro and with stable microtubules in mitotic spindles of cultured cells. *EMBO J.* **9**, 4095-4102.
Markova, M. D. (2004). Electron microscopic observations of human sperm whole-mounts after extraction for nuclear matrix and intermediate filaments (NM-IF). *Int. J. Androl.* **27**, 291-295.
Marshall, W. F. (2009). Centriole evolution. *Curr. Opin. Cell Biol.* **21**, 14-19.
Marshall, W. F. and Rosenbaum, J. L. (2001). Intraflagellar transport balances continuous turnover of outer doublet microtubules: implications for flagellar length control. *J. Cell Biol.* **155**, 405-414.
Marshall, W. F., Qin, H., Rodrigo Brenni, M. and Rosenbaum, J. L. (2005). Flagellar length control system: testing a simple model based on intraflagellar transport and turnover. *Mol. Biol. Cell* **16**, 270-278.
Miyoshi, K., Kasahara, K., Miyazaki, I. and Asanuma, M. (2011). Factors that influence primary cilium length. *Acta Med. Okayama* **65**, 279-285.

Nielsen, M. G., Turner, F. R., Hutchens, J. A. and Raff, E. C. (2001). Axoneme-specific β-tubulin specialization: a conserved C-terminal motif specifies the central pair. *Curr. Biol.* **11**, 529-533.
Nogales-Cadenas, R., Abascal, F., Díez-Pérez, J., Carazo, J. M. and Pascual-Montano, A. (2009). CentrosomeDB: a human centrosomal proteins database. *Nucleic Acids Res.* **37**, D175-D180.
Oh, E. C. and Katsanis, N. (2012). Cilia in vertebrate development and disease. *Development* **139**, 443-448.
Pease, D. C. (1963). The ultrastructure of flagellar fibrils. *J. Cell Biol.* **18**, 313-326.
Pirollet, F., Rauch, C. T., Job, D. and Margolis, R. L. (1989). Monoclonal antibody to microtubule-associated STOP protein: affinity purification of neuronal STOP activity and comparison of antigen with activity in neuronal and nonneuronal cell extracts. *Biochemistry* **28**, 835-842.
Platt, M. D., Salicioni, A. M., Hunt, D. F. and Visconti, P. E. (2009). Use of differential isotopic labeling and mass spectrometry to analyze capacitation-associated changes in the phosphorylation status of mouse sperm proteins. *J. Proteome Res.* **8**, 1431-1440.
Quinones, G. B., Danowski, B. A., Devaraj, A., Singh, V. and Ligon, L. A. (2011). The posttranslational modification of tubulin undergoes a switch from detyrosination to acetylation as epithelial cells become polarized. *Mol. Biol. Cell* **22**, 1045-1057.
Sathananthan, A. H. (2013). Ultrastructure of human gametes, fertilization and embryos in assisted reproduction: a personal survey. *Micron* **44**, 1-20.
Sathananthan, A. H., Ratnam, S. S., Ng, S. C., Tarín, J. J., Gianaroli, L. and Trounson, A. (1996). The sperm centriole: its inheritance, replication and perpetuation in early human embryos. *Hum. Reprod.* **11**, 345-356.
Schlingmann, K., Michaut, M. A., McElwee, J. L., Wolff, C. A., Travis, A. J. and Turner, R. M. (2007). Calmodulin and CaMKII in the sperm principal piece: evidence for a motility-related calcium/calmodulin pathway. *J. Androl.* **28**, 706-716.
Schwenk, B. M., Lang, C. M., Hogl, S., Tahirovic, S., Orozco, D., Rentzsch, K., Lichtenthaler, S. F., Hoogenraad, C. C., Capell, A., Haass, C. et al. (2014). The FTLD risk factor TMEM106B and MAP6 control dendritic trafficking of lysosomes. *EMBO J.* **33**, 450-467.
Snyder, J. A. and McIntosh, J. R. (1976). Biochemistry and physiology of microtubules. *Annu. Rev. Biochem.* **45**, 699-720.
Steffen, W. and Linck, R. W. (1988). Evidence for tektins in centrioles and axonemal microtubules. *Proc. Natl. Acad. Sci. USA* **85**, 2643-2647.
Takeda, S. and Narita, K. (2012). Structure and function of vertebrate cilia, towards a new taxonomy. *Differentiation* **83**, S4-S11.
Tran, J. Q., Li, C., Chyan, A., Chung, L. and Morrissette, N. S. (2012). SPM1 stabilizes subpellicular microtubules in Toxoplasma gondii. *Eukaryot. Cell* **11**, 206-216.
Uhlen, M., Oksvold, P., Fagerberg, L., Lundberg, E., Jonasson, K., Forsberg, M., Zwahlen, M., Kampf, C., Wester, K., Hober, S. et al. (2010). Towards a knowledge-based Human Protein Atlas. *Nat. Biotechnol.* **28**, 1248-1250.
Volle, J., Brocard, J., Saoud, M., Gory-Faure, S., Brunelin, J., Andrieux, A. and Suaud-Chagny, M. F. (2013). Reduced expression of STOP/MAP6 in mice leads to cognitive deficits. *Schizophr. Bull.* **39**, 969-978.
Woods, A., Sherwin, T., Sasse, R., MacRae, T. H., Baines, A. J. and Gull, K. (1989). Definition of individual components within the cytoskeleton of Trypanosoma brucei by a library of monoclonal antibodies. *J. Cell Sci.* **93**, 491-500.

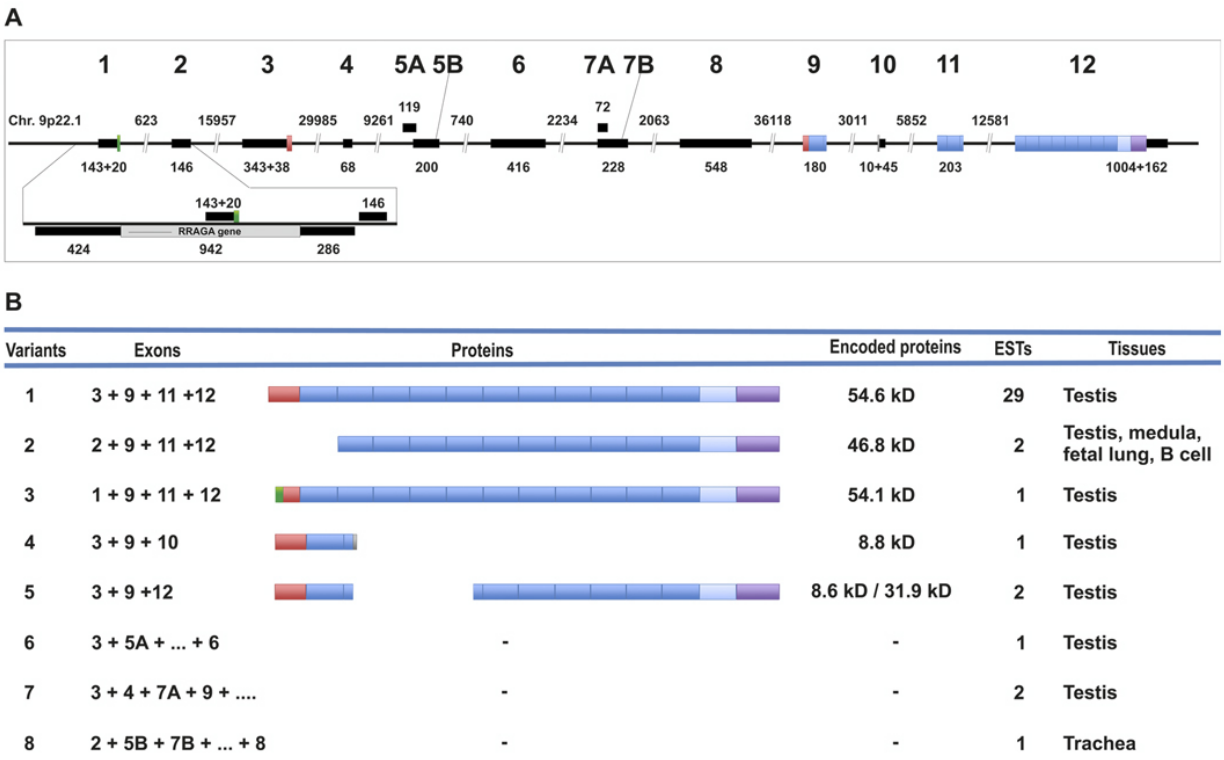

Fig. S1: Schematic representations of the *HsSAXO1* gene, mRNA variants and corresponding proteins. A. Schematic representation of the *HsSAXO1* gene chromosomal locus (thin line) with the exonic non-coding (black thick lines) and coding (large boxes) elements reported. Zoom: the single exon of the RRAGA gene is located on the opposite strand, with the coding sequence (light gray) overlapping *HsSAXO1* exon 1. Exons 5 and 7 represent 5' or 3' alternative splicing sites, respectively. Size of introns, coding and non-coding sequences are indicated in bp. Blue: Mn-like modules. Asterisk: vertebrate specific CPASYpsPPG motif. Red: cysteine-rich N-terminal domain. Green: alternatively used N- terminal domains. **B.** Sequence analysis of genomic, EST and cDNA databases identified 8 putative isoforms with isoform 1 being the most represented (29 ESTs), encoding a 54.6 kD protein. The 7 other isoforms are only represented by one or two ESTs potentially encoding proteins ranging from 8.6 kD to 54.1 kD (isoforms 2 to 5), whilst it was difficult to define a coding sequence for isoforms 6 to 8 as only very short ORFs were present. The N-terminal cysteine-rich domain (red boxes) present in isoforms 1, 4, and 5, is partially replaced by a non-related domain in isoform 3 (green box) or absent in isoform 2. The variation in the repeat number (12 in isoforms 1 and 3, 11 in isoform 2, and only one in isoforms 4 and 5 (blue boxes), conjugated to shuffling N-terminal domain, suggests distinct and specific functions among the putative *Hs*SAXO1 isoforms.

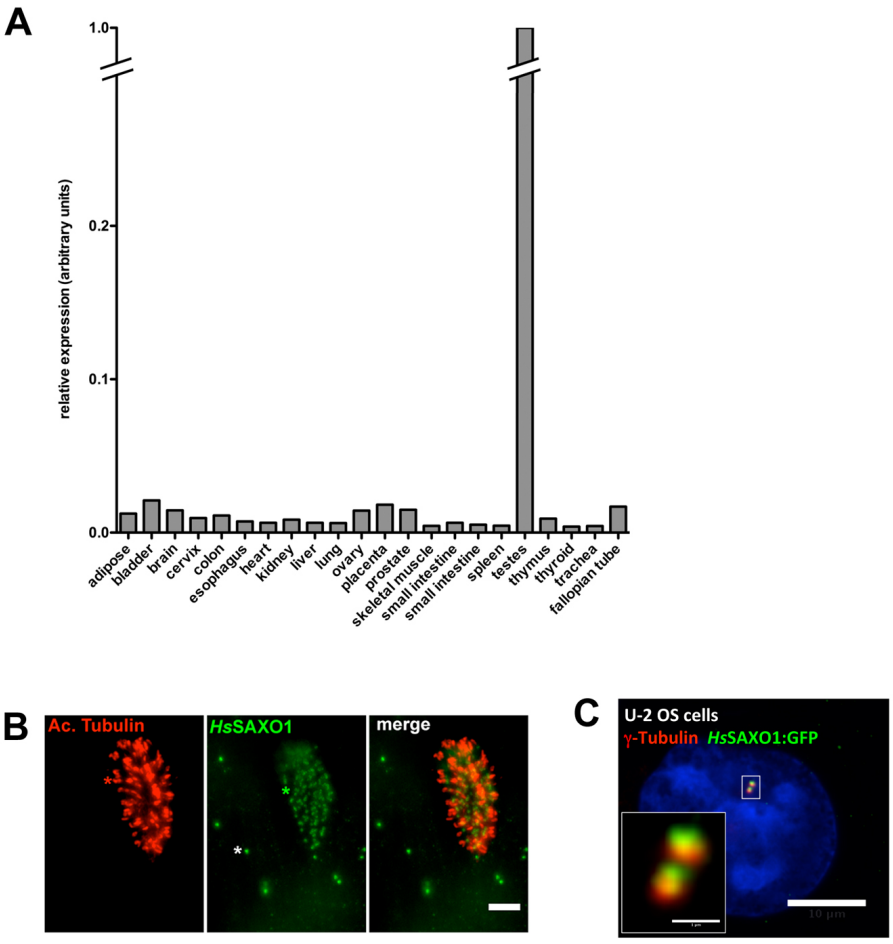

Fig. S2: A. RT-qPCR on total RNA from Human tissues. RT-qPCR was performed on 20 ng of total RNA from different human tissues. C_T values for *HsSAXO1* expression level were normalized for expression of 2 housekeeping genes in each tissue (*GAPDH* and *β2microglobulin*). *HsSAXO1* expression level was then expressed relative to level in testes, the highest expressing tissue. All tissues tested expressed *HsSAXO1* although to a much lesser extent compared to testes (50 to 250 fold less). These data correlate with the IF data showing that all tested cells express *Hs*SAXO1 mainly at the centrosome (and basal bodies in ciliated cells) whereas the protein is found along the 50 µm long flagellum in sperm cells. These data are also consistent with the fact that *Hs*SAXO1 could be detected in WB only in sperm extracts. **B.** Immuno-labelling of *Hs*SAXO1 in human bronchial epithelial cells (HBECs). In multi-ciliated cells *Hs*SAXO1 (green) localizes to the basal bodies, and to the centrosome in non-ciliated cells. Cilia are labelled with anti-acetylated tubulin (red). Red asterisk: cilia; white asterisk: centrioles; green asterisk: basal bodies. Scale bar represents 10 µm. **C.** *Hs*SAXO1:GFP localizes at the centrioles. *Hs*SAXO1:GFP and γ-Tubulin co-localized in transfected U-2 OS cells. *Hs*SAXO1:GFP (direct GFP fluorescence, green) localizes at the centrioles together with γ-Tubulin (immuno-labelled, red). Nuclei were stained with DAPI. Scale bars represent 10 µm and 1 µm (inset).

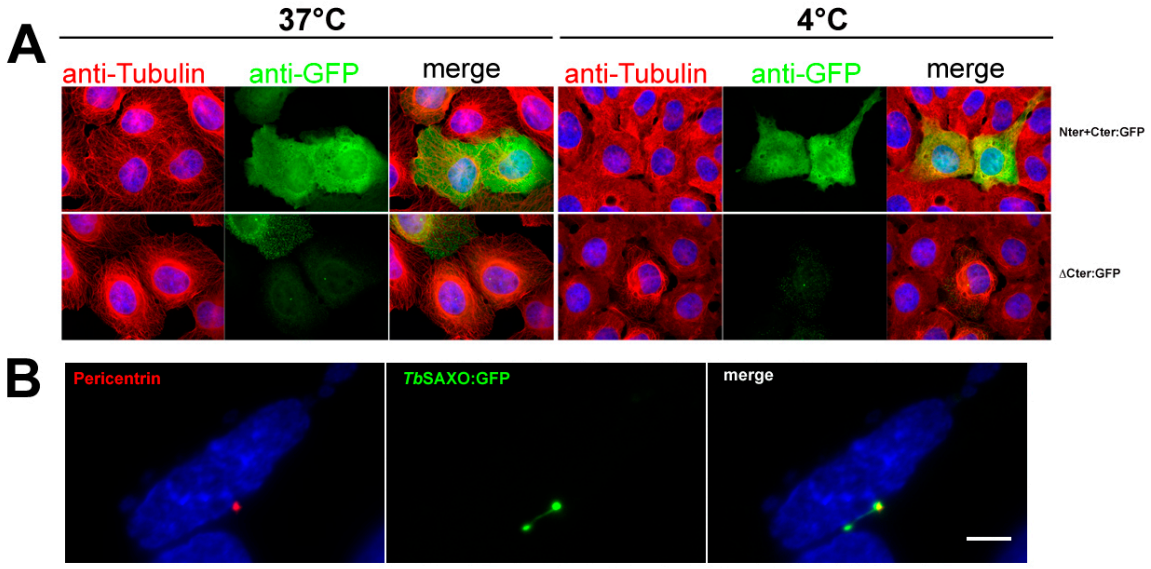

Fig. S3. A. Ectopic expression and localization of Nter+Cter:GFP and ΔCter:GFP in U-2 OS cells. Ectopic expression of Nter+Cter:GFP and ΔCter:GFP in U-2 OS cells that were mock-treated (37°C) or cold-treated (4°C), fixed, and labelled with anti-GFP (green) and anti-α-tubulin (red). **B.** Expression of *Tb*SAXO:GFP in ciliated RPE1 cells. Ciliated RPE1 expressing *Tb*SAXO:GFP co-labelled with anti-pericentrin (red) and anti-GFP (green). Bar represents 5 μm.

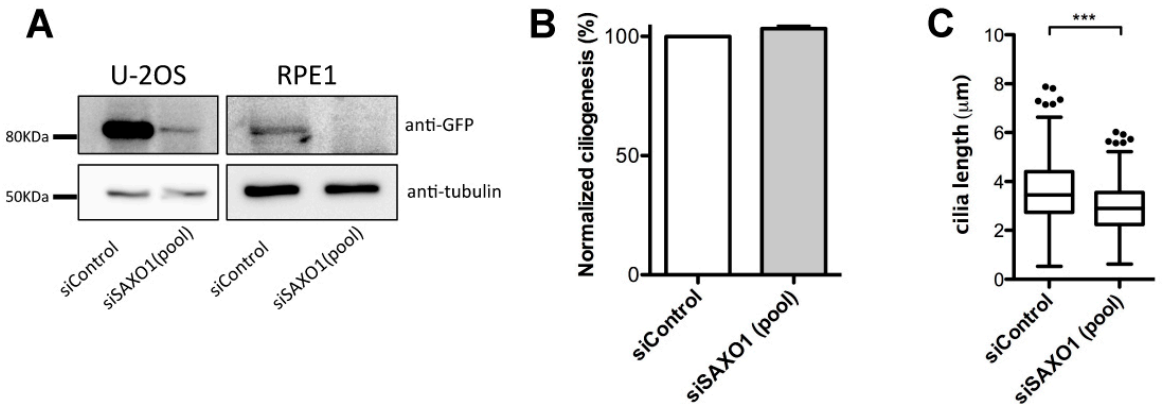

Fig. S4. siRNA knockdown of *Hs*SAXO1 identifies a role in cilia length. A. Western-blot of U-2OS and RPE1 cells expressing *Hs*SAXO1:GFP and siControl or siSAXO1(pool) treated for 48 h. Membranes were probed with anti-GFP (top), striped then probed with anti-tubulin (bottom). **B**. Percentage of ciliated cells in siSAXO1(pool) treated RPE1 cells compared to siControl treated cells. **C.** Tukey's Box and Wiskers plot of cilia length in siControl or siSAXO1(pool) treated RPE1 cells. Average cilia length was 3.61±0.07 μm in siControl samples and 2.95±0.06 μm in siSAXO1(pool) samples. *** P<0.001. Over 3 independent experiments, n=285, and n=287 for siControl and siSAXO1(pool) respectively.

Table S1. Accession numbers for the proteins used in MEME analysis.

Download Table S1

Table S2. Isoform and tissue distributions among HsSAXO1 ESTs in databases.

Download Table S2

Table S3. Primer sequences

End-point RT-PCR	**Primer pair sequence**
*Hs*SAXO1	5'-CTACAAGCAGTGGTCCAGCA-3' 5'-TCCTGTGACCCAAAGCATCC-3'
Human actin (BC002409)	5'-TGGGACGACATGGAGAAAA-3' 5'-AAGGAAGGCTGGAAGAGTGC-3'

RT-qPCR	**Primer pair sequence**
*Hs*SAXO1	5'-CACCACTCGGGCCCACTAT-3' 5'-GGCCAGACCAATGAGGCTTAC-3'
GAPDH	5'-CACCCATGGCAAATTCC-3' 5'-TGGGATTTCCATTGATGACAAG-3'
2-microglobulin	5'- GTGCTGTCTCCATGTTTGATGTATC -3' 5'- CTAAGTTGCCAGCCCTCCTAGA -3'

siRNA	
HsSAXO1	1) CCACACACCAGGACGAUUA **siSAXO1(1)** 2) UGGAUUUGCUCACGACGUA **siSAXO1(2)** 3) CAGUGAAGGUCCACCAGUA 4) CACAAAUACCAGCCGGCAU
Non-targeting control (pool)	1) UGGUUUACAUGUCGACUAA 2) UGGUUUACAUGUUGUGUGA 3) UGGUUUACAUGUUUUCUGA 4) UGGUUUACAUGUUUUCCUA